13

General Formula for On-Axis Sun-Tracking System

Kok-Keong Chong, Chee-Woon Wong
Universiti Tunku Abdul Rahman
Malaysia

1. Introduction

Sun-tracking system plays an important role in the development of solar energy applications, especially for the high solar concentration systems that directly convert the solar energy into thermal or electrical energy. High degree of sun-tracking accuracy is required to ensure that the solar collector is capable of harnessing the maximum solar energy throughout the day. High concentration solar power systems, such as central receiver system, parabolic trough, parabolic dish etc, are the common in the applications of collecting solar energy. In order to maintain high output power and stability of the solar power system, a high-precision sun-tracking system is necessary to follow the sun's trajectory from dawn until dusk.

For achieving high degree of tracking accuracy, sun-tracking systems normally employ sensors to feedback error signals to the control system for continuously receiving maximum solar irradiation on the receiver. Over the past two decades, various strategies have been proposed and they can be classified into the following three categories, i.e. open-loop, closed-loop and hybrid sun-tracking (Lee et al., 2009). In the open-loop tracking approach, the control program will perform calculation to identify the sun's path using a specific sun-tracking formula in order to drive the solar collector towards the sun. Open-loop sensors are employed to determine the rotational angles of the tracking axes and guarantee that the solar collector is positioned at the right angles. On the other hand, for the closed-loop tracking scheme, the solar collector normally will sense the direct solar radiation falling on a closed-loop sensor as a feedback signal to ensure that the solar collector is capable of tracking the sun all the time. Instead of the above options, some researchers have also designed a hybrid system that contains both the open-loop and closed-loop sensors to attain a good tracking accuracy. The above-mentioned tracking methods are operated by either a microcontroller based control system or a PC based control system in order to trace the position of the sun.

Azimuth-elevation and tilt-roll tracking mechanisms are among the most commonly used sun-tracking methods for aiming the solar collector towards the sun at all times. Each of these two sun-tracking methods has its own specific sun-tracking formula and they are not interrelated in many decades ago. In this chapter, the most general form of sun-tracking formula that embraces all the possible on-axis tracking approaches is derived and presented in details. The general sun-tracking formula not only can provide a general mathematical solution, but more significantly, it can improve the sun-tracking accuracy by tackling the

installation error of the solar collector. The precision of foundation alignment during the installation of solar collector becomes tolerable because any imprecise configuration in the tracking axes can be easily compensated by changing the parameters' values in the general sun-tracking formula. By integrating the novel general formula into the open-loop sun-tracking system, this strategy is definitely a cost effective way to be capable of remedying the installation error of the solar collector with a significant improvement in the tracking accuracy.

2. Overview of sun-tracking systems

2.1 Sun-tracking approaches

A good sun-tracking system must be reliable and able to track the sun at the right angle even in the periods of cloud cover. Over the past two decades, various types of sun-tracking mechanisms have been proposed to enhance the solar energy harnessing performance of solar collectors. Although the degree of accuracy required depends on the specific characteristics of the solar concentrating system being analyzed, generally the higher the system concentration the higher the tracking accuracy will be needed (Blanco-Muriel et al., 2001).

In this section, we would like to briefly review the three categories of sun-tracking algorithms (i.e. open-loop, closed-loop and hybrid) with some relevant examples. For the closed-loop sun-tracking approach, various active sensor devices, such as CCD sensor or photodiode sensor are utilized to sense the position of the solar image on the receiver and a feedback signal is then generated to the controller if the solar image moves away from the receiver. Sun-tracking systems that employ active sensor devices are known as closed-loop sun trackers. Although the performance of the closed-loop tracking system is easily affected by weather conditions and environmental factors, it has allowed savings in terms of cost, time and effort by omitting more precise sun tracker alignment work. In addition, this strategy is capable of achieving a tracking accuracy in the range of a few milli-radians (mrad) during fine weather. For that reason, the closed-loop tracking approach has been traditionally used in the active sun-tracking scheme over the past 20 years (Arbab et al., 2009; Berenguel et al., 2004; Kalogirou, 1996; Lee et al., 2006). For example, Kribus et al. (2004) designed a closed-loop controller for heliostats, which improved the pointing error of the solar image up to 0.1 mrad, with the aid of four CCD cameras set on the target. However, this method is rather expensive and complicated because it requires four CCD cameras and four radiometers to be placed on the target. Then the solar images captured by CCD cameras must be analysed by a computer to generate the control correction feedback for correcting tracking errors. In 2006, Luque-Heredia et al. (2006) presented a sun-tracking error monitoring system that uses a monolithic optoelectronic sensor for a concentrator photovoltaic system. According to the results from the case study, this monitoring system achieved a tracking accuracy of better than 0.1^{o}. However, the criterion is that this tracking system requires full clear sky days to operate, as the incident sunlight has to be above a certain threshold to ensure that the minimum required resolution is met. That same year, Aiuchi et al. (2006) developed a heliostat with an equatorial mount and a closed-loop photo-sensor control system. The experimental results showed that the tracking error of the heliostat was estimated to be 2 mrad during fine weather. Nevertheless, this tracking method is not popular and only can be used for sun trackers with an equatorial mount configuration, which is not a common tracker mechanical structure and is complicated

because the central of gravity for the solar collector is far off the pedestal. Furthermore, Chen et al. (2006, 2007) presented studies of digital and analogue sun sensors based on the optical vernier and optical nonlinear compensation measuring principle respectively. The proposed digital and analogue sun sensors have accuracies of 0.02^{o} and 0.2^{o} correspondingly for the entire field of view of ±64° and ±62° respectively. The major disadvantage of these sensors is that the field of view, which is in the range of about ±64° for both elevation and azimuth directions, is rather small compared to the dynamic range of motion for a practical sun tracker that is about ±70° and ±140° for elevation and azimuth directions, respectively. Besides that, it is just implemented at the testing stage in precise sun sensors to measure the position of the sun and has not yet been applied in any closed-loop sun-tracking system so far.

Although closed-loop sun-tracking system can produce a much better tracking accuracy, this type of system will lose its feedback signal and subsequently its track to the sun position when the sensor is shaded or when the sun is blocked by clouds. As an alternative method to overcome the limitation of closed-loop sun trackers, open-loop sun trackers were introduced by using open-loop sensors that do not require any solar image as feedback. The open-loop sensor such as encoder will ensure that the solar collector is positioned at pre-calculated angles, which are obtained from a special formula or algorithm. Referring to the literatures (Blanco-Muriel et al., 2001; Grena, 2008; Meeus, 1991; Reda & Andreas, 2004; Sproul, 2007), the sun's azimuth and elevation angles can be determined by the sun position formula or algorithm at the given date, time and geographical information. This tracking approach has the ability to achieve tracking error within ±0.2° when the mechanical structure is precisely made as well as the alignment work is perfectly done. Generally, these algorithms are integrated into the microprocessor based or computer based controller. In 2004, Abdallah and Nijmeh (2004) designed a two axes sun tracking system, which is operated by an open-loop control system. A programmable logic controller (PLC) was used to calculate the solar vector and to control the sun tracker so that it follows the sun's trajectory. In addition, Shanmugam & Christraj (2005) presented a computer program written in *Visual Basic* that is capable of determining the sun's position and thus drive a paraboloidal dish concentrator (PDS) along the East-West axis or North-South axis for receiving maximum solar radiation.

In general, both sun-tracking approaches mentioned above have both strengths and drawbacks, so some hybrid sun-tracking systems have been developed to include both the open-loop and closed-loop sensors for the sake of high tracking accuracy. Early in the 21st century, Nuwayhid et al. (2001) adopted both the open-loop and closed-loop tracking methods into a parabolic concentrator attached to a polar tracking system. In the open-loop scheme, a computer acts as controller to calculate two rotational angles, i.e. solar declination and hour angles, as well as to drive the concentrator along the declination and polar axes. In the closed-loop scheme, nine light-dependent resistors (LDR) are arranged in an array of a circular-shaped "iris" to facilitate sun-tracking with a high degree of accuracy. In 2004, Luque-Heredia et al. (2004) proposed a novel *PI* based hybrid sun-tracking algorithm for a concentrator photovoltaic system. In their design, the system can act in both open-loop and closed-loop mode. A mathematical model that involves a time and geographical coordinates function as well as a set of disturbances provides a feed-forward open-loop estimation of the sun's position. To determine the sun's position with high precision, a feedback loop was introduced according to the error correction routine, which is derived from the estimation of the error of the sun equations that are caused by external disturbances at the present stage based on its

historical path. One year later, Rubio et al. (2007) fabricated and evaluated a new control strategy for a photovoltaic (PV) solar tracker that operated in two tracking modes, i.e. normal tracking mode and search mode. The normal tracking mode combines an open-loop tracking mode that is based on solar movement models and a closed-loop tracking mode that corresponds to the electro-optical controller to obtain a sun-tracking error, which is smaller than a specified boundary value and enough for solar radiation to produce electrical energy. Search mode will be started when the sun-tracking error is large or no electrical energy is produced. The solar tracker will move according to a square spiral pattern in the azimuth-elevation plane to sense the sun's position until the tracking error is small enough.

2.2 Types of sun trackers

Taking into consideration of all the reviewed sun-tracking methods, sun trackers can be grouped into one-axis and two-axis tracking devices. Fig. 1 illustrates all the available types of sun trackers in the world. For one-axis sun tracker, the tracking system drives the collector about an axis of rotation until the sun central ray and the aperture normal are coplanar. Broadly speaking, there are three types of one-axis sun tracker:

1. **Horizontal-Axis Tracker** – the tracking axis is to remain parallel to the surface of the earth and it is always oriented along East-West or North-South direction.
2. **Tilted-Axis Tracker** – the tracking axis is tilted from the horizon by an angle oriented along North-South direction, e.g. Latitude-tilted-axis sun tracker.
3. **Vertical-Axis Tracker** – the tracking axis is collinear with the zenith axis and it is known as azimuth sun tracker.

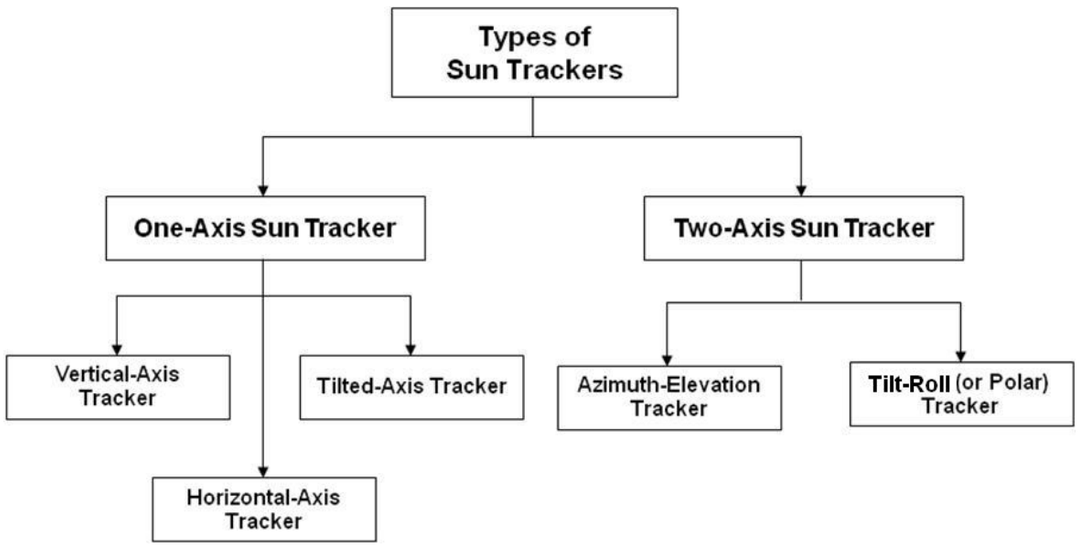

Fig. 1. Types of sun trackers

In contrast, the two-axis sun tracker, such as azimuth-elevation and tilt-roll sun trackers, tracks the sun in two axes such that the sun vector is normal to the aperture as to attain 100% energy collection efficiency. Azimuth-elevation and tilt-roll (or polar) sun tracker are the most popular two-axis sun tracker employed in various solar energy applications. In the azimuth-elevation sun-tracking system, the solar collector must be free to rotate about the azimuth and the elevation axes. The primary tracking axis or azimuth axis must parallel to

the zenith axis, and elevation axis or secondary tracking axis always orthogonal to the azimuth axis as well as parallel to the earth surface. The tracking angle about the azimuth axis is the solar azimuth angle and the tracking angle about the elevation axis is the solar elevation angle. Alternatively, tilt-roll (or polar) tracking system adopts an idea of driving the collector to follow the sun-rising in the east and sun-setting in the west from morning to evening as well as changing the tilting angle of the collector due to the yearly change of sun path. Hence, for the tilt-roll tracking system, one axis of rotation is aligned parallel with the earth's polar axis that is aimed towards the star Polaris. This gives it a tilt from the horizon equal to the local latitude angle. The other axis of rotation is perpendicular to this polar axis. The tracking angle about the polar axis is equal to the sun's hour angle and the tracking angle about the perpendicular axis is dependent on the declination angle. The advantage of tilt-roll tracking is that the tracking velocity is almost constant at 15 degrees per hour and therefore the control system is easy to be designed.

2.3 The challenges of sun-tracking systems

In fact, the tracking accuracy requirement is very much reliant on the design and application of the solar collector. In this case, the longer the distance between the solar concentrator and the receiver the higher the tracking accuracy required will be because the solar image becomes more sensitive to the movement of the solar concentrator. As a result, a heliostat or off-axis sun tracker normally requires much higher tracking accuracy compared to that of on-axis sun tracker for the reason that the distance between the heliostat and the target is normally much longer, especially for a central receiver system configuration. In this context, a tracking accuracy in the range of a few miliradians (mrad) is in fact sufficient for an on-axis sun tracker to maintain its good performance when highly concentrated sunlight is involved (Chong et al, 2010). Despite having many existing on-axis sun-tracking methods, the designs available to achieve a good tracking accuracy of a few mrad are complicated and expensive. It is worthwhile to note that conventional on-axis sun-tracking systems normally adopt two common configurations, which are azimuth-elevation and tilt-roll (polar tracking), limited by the available basic mathematical formulas of sun-tracking system. For azimuth-elevation tracking system, the sun-tracking axes must be strictly aligned with both zenith and real north. For a tilt-roll tracking system, the sun-tracking axes must be exactly aligned with both latitude angle and real north. The major cause of sun-tracking errors is how well the aforementioned alignment can be done and any installation or fabrication defect will result in low tracking accuracy. According to our previous study for the azimuth-elevation tracking system, a misalignment of azimuth shaft relative to zenith axis of 0.4° can cause tracking error ranging from 6.45 to 6.52 mrad (Chong & Wong, 2009). In practice, most solar power plants all over the world use a large solar collector area to save on manufacturing cost and this has indirectly made the alignment work of the sun-tracking axes much more difficult. In this case, the alignment of the tracking axes involves an extensive amount of heavy-duty mechanical and civil works due to the requirement for thick shafts to support the movement of a large solar collector, which normally has a total collection area in the range of several tens of square meters to nearly a hundred square meters. Under such tough conditions, a very precise alignment is really a great challenge to the manufacturer because a slight misalignment will result in significant sun-tracking errors. To overcome this problem, an unprecedented on-axis general sun-tracking formula has been proposed to allow the sun tracker to track the sun in any two arbitrarily orientated tracking

axes (Chong & Wong, 2009). In this chapter, we would like to introduce a novel sun-tracking system by integrating the general formula into the sun-tracking algorithm so that we can track the sun accurately and cost effectively, even if there is some misalignment from the ideal azimuth-elevation or tilt-roll configuration. In the new tracking system, any misalignment or defect can be rectified without the need for any drastic or labor-intensive modifications to either the hardware or the software components of the tracking system. In other words, even though the alignments of the azimuth-elevation axes with respect to the zenith-axis and real north are not properly done during the installation, the new sun-tracking algorithm can still accommodate the misalignment by changing the values of parameters in the tracking program. The advantage of the new tracking algorithm is that it can simplify the fabrication and installation work of solar collectors with higher tolerance in terms of the tracking axes alignment. This strategy has allowed great savings in terms of cost, time and effort by omitting complicated solutions proposed by other researchers such as adding a closed-loop feedback controller or a flexible and complex mechanical structure to level out the sun-tracking error (Chen et al., 2001; Luque-Heredia et al., 2007).

3. General formula for on-axis sun-tracking system

A novel general formula for on-axis sun-tracking system has been introduced and derived to allow the sun tracker to track the sun in two orthogonal driving axes with any arbitrary orientation (Chong & Wong, 2009). Chen et al. (2006) was the pioneer group to derive a general sun-tracking formula for heliostats with arbitrarily oriented axes. The newly derived general formula by Chen et al. (2006) is limited to the case of off-axis sun tracker (heliostat) where the target is fixed on the earth surface and hence a heliostat normal vector must always bisect the angle between a sun vector and a target vector. As a complimentary to Chen's work, Chong and Wong (2009) derive the general formula for the case of on-axis sun tracker where the target is fixed along the optical axis of the reflector and therefore the reflector normal vector must be always parallel with the sun vector. With this complete mathematical solution, the use of azimuth-elevation and tilt-roll tracking formulas are the special case of it.

3.1 Derivation of general formula

Prior to mathematical derivation, it is worthwhile to state that the task of the on-axis sun-tracking system is to aim a solar collector towards the sun by turning it about two perpendicular axes so that the sunray is always normal relative to the collector surface. Under this circumstance, the angles that are required to move the solar collector to this orientation from its initial orientation are known as sun-tracking angles. In the derivation of sun-tracking formula, it is necessary to describe the sun's position vector and the collector's normal vector in the same coordinate reference frame, which is the collector-centre frame. Nevertheless, the unit vector of the sun's position is usually described in the earth-centre frame due to the sun's daily and yearly rotational movements relative to the earth. Thus, to derive the sun-tracking formula, it would be convenient to use the coordinate transformation method to transform the sun's position vector from earth-centre frame to earth-surface frame and then to collector-centre frame. By describing the sun's position vector in the collector-centre frame, we can resolve it into solar azimuth and solar altitude angles relative to the solar collector and subsequently the amount of angles needed to move the solar collector can be determined easily.

According to Stine & Harrigan (1985), the sun's position vector relative to the earth-centre frame can be defined as shown in Fig. 2, where CM, CE and CP represent three orthogonal axes from the centre of earth pointing towards the meridian, east and Polaris respectively. The unified vector for the sun position ***S*** in the earth-centre frame can be written in the form of direction cosines as follow:

$$\boldsymbol{S} = \begin{bmatrix} S_M \\ S_E \\ S_P \end{bmatrix} = \begin{bmatrix} \cos\delta\cos\omega \\ -\cos\delta\sin\omega \\ \sin\delta \end{bmatrix} \tag{1}$$

where δ is the declination angle and ω is hour angle are defined as follow (Stine & Harrigan, 1985): The accuracy of the declination angles is important in navigation and astronomy. However, an approximation accurate to within 1 degree is adequate in many solar purposes. One such approximation for the declination angle is

$$\delta = \sin^{-1}\{0.39795 \cos [0.98563 (N-173)]\} \quad \text{(degrees)} \tag{2}$$

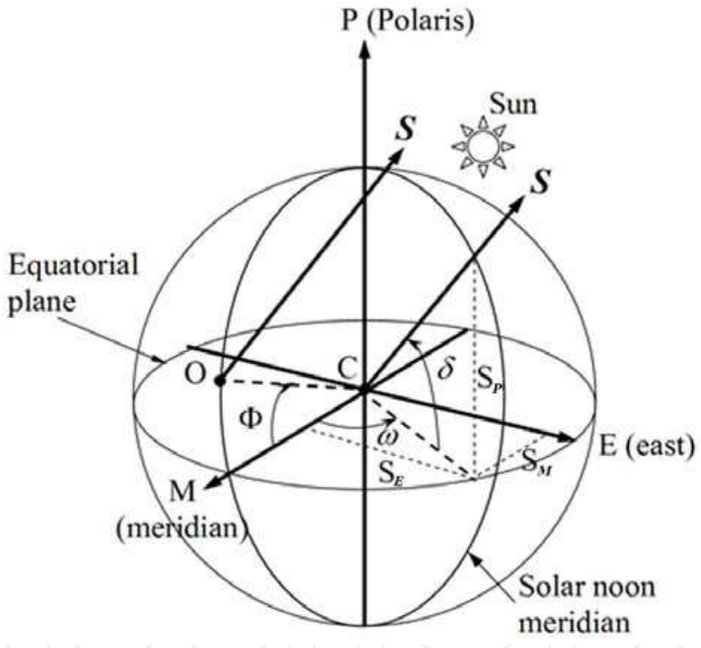

Fig. 2. The sun's position vector relative to the earth-centre frame. In the earth-centre frame, CM, CE and CP represent three orthogonal axes from the centre of the earth pointing towards meridian, east and Polaris, respectively

where N is day number and calendar dates are expressed as the N = 1, starting with January 1. Thus March 22 would be N = 31 + 28 + 22 = 81 and December 31 means N = 365.

The hour angle expresses the time of day with respect to the solar noon. It is the angle between the planes of the meridian-containing observer and meridian that touches the earth-sun line. It is zero at solar noon and increases by 15° every hour:

$$\omega = 15(t_s - 12) \quad \text{(degrees)} \tag{3}$$

where t_s is the solar time in hours. A solar time is a 24-hour clock with 12:00 as the exact time when the sun is at the highest point in the sky. The concept of solar time is to predict the direction of the sun's ray relative to a point on the earth. Solar time is location or longitudinal dependent. It is generally different from local clock time *(LCT) (*defined by politically time zones)

Fig. 3 depicts the coordinate system in the earth-surface frame that comprises of OZ, OE and ON axes, in which they point towards zenith, east and north respectively. The detail of coordinate transformation for the vector ***S*** from earth-centre frame to earth-surface frame was presented by Stine & Harrigan (1985) and the needed transformation matrix for the above coordinate transformation can be expressed as

$$\left[\Phi\right]=\begin{bmatrix}\cos\Phi & 0 & \sin\Phi\\ 0 & 1 & 0\\ -\sin\Phi & 0 & \cos\Phi\end{bmatrix} \tag{4}$$

where Φ is the latitude angle.

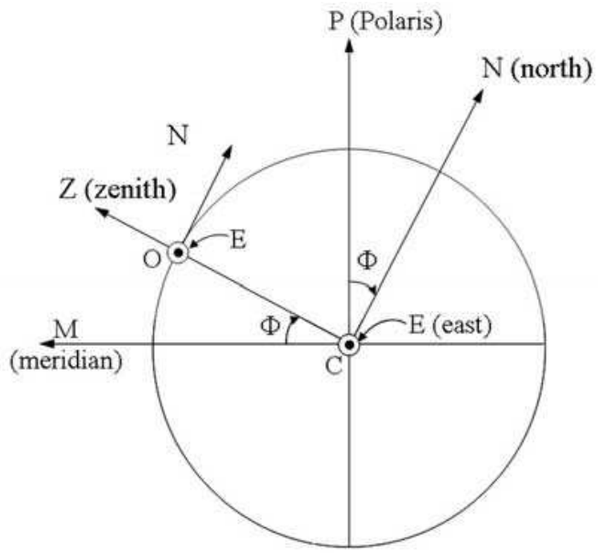

Fig. 3. The coordinate system in the earth-surface frame that consists of OZ, OE and ON axes, in which they point towards zenith, east and north respectively. The transformation of the vector S from earth-centre frame to earth-surface frame can be obtained through a rotation angle that is equivalent to the latitude angle (Φ)

Now, let us consider a new coordinate system that is defined by three orthogonal coordinate axes in the collector-centre frame as shown in Fig. 4. For the collector-centre frame, the origin O is defined at the centre of the collector surface and it coincides with the origin of earth-surface frame. OV is defined as vertical axis in this coordinate system and it is parallel with first rotational axis of the solar collector. Meanwhile, OR is named as reference axis in which one of the tracking angle β is defined relative to this axis. The third orthogonal axis, OH, is named as horizontal axis and it is parallel with the initial position of the second rotational axis. The OR and OH axes form the level plane where the collector surface is driven relative to this plane. Fig. 4 also reveals the simplest structure of solar collector that

can be driven in two rotational axes: the first rotational axis that is parallel with OV and the second rotational axis that is known as EE′ dotted line (it can rotate around the first axis during the sun-tracking but must always be perpendicular with the first axis). From Fig. 4, θ is the amount of rotational angle about EE′ axis measured from OV axis, whereas β is the rotational angle about OV axis measured from OR axis. Furthermore, α is solar altitude angle in the collector-centre frame, which is equal to $\pi/2-\theta$. In the collector-centre frame, the sun position $\boldsymbol{S}'$ can be written in the form of direction cosines as follow:

$$\boldsymbol{S}' = \begin{bmatrix} S_V \\ S_H \\ S_R \end{bmatrix} = \begin{bmatrix} \sin\alpha \\ \cos\alpha\sin\beta \\ \cos\alpha\cos\beta \end{bmatrix} \tag{5}$$

In an ideal azimuth-elevation system, OV, OH and OR axes of the collector-centre frame are parallel with OZ, OE and ON axes of the earth-surface frame accordingly as shown in Fig. 5. To generalize the mathematical formula from the specific azimuth-elevation system to any arbitrarily oriented sun-tracking system, the orientations of OV, OH and OR axes will be described by three tilted angles relative to the earth-surface frame. Three tilting angles have been introduced here because the two-axis mechanical drive can be arbitrarily oriented about any of the three principal axes of earth-surface frame: ϕ is the rotational angle about zenith-axis if the other two angles are null, λ is the rotational angle about north-axis if the other two angles are null and ζ is the rotational angle about east-axis if the other two angles are null. On top of that, the combination of the above-mentioned angles can further generate more unrepeated orientations of the two tracking axes in earth-surface frame, which is very important in later consideration for improving sun-tracking accuracy of solar collector.

Fig. 6(a) – (c) show the process of how the collector-centre frame is tilted step-by-step relative to the earth-surface frame, where OV′, OH′ and OR′ axes represent the intermediate position for OV, OH and OR axes, respectively. In Fig. 6(a), the first tilted angle, $+\phi$, is a rotational angle about the OZ axis in clockwise direction. In Fig. 6(b), the second tilted angle, $-\lambda$, is a rotational angle about OR′ axis in counter-clockwise direction. Lastly, in Fig. 6(c), the third tilted angle, $+\zeta$, is a rotational angle about OH axis in clockwise direction. Fig. 7 shows the combination of the above three rotations in 3D view for the collector-centre frame relative to the earth-surface frame, where the change of coordinate system for each axis follows the order: $Z \rightarrow V' \rightarrow V$, $E \rightarrow H' \rightarrow H$ and $N \rightarrow R' \rightarrow R$. Similar to the latitude angle, in the direction representation of the three tilting angles, we define positive sign to the angles, i.e. ϕ, λ, ζ, for the rotation in the clockwise direction. In other words, clockwise and counter-clockwise rotations can be named as positive and negative rotations respectively.

As shown in Fig. 6(a) – (c), the transformation matrices correspond to the three tilting angles (ϕ, λ and ζ) can be obtained accordingly as follow:

$$[\phi] = \begin{bmatrix} 1 & 0 & 0 \\ 0 & \cos\phi & -\sin\phi \\ 0 & \sin\phi & \cos\phi \end{bmatrix} \tag{6a}$$

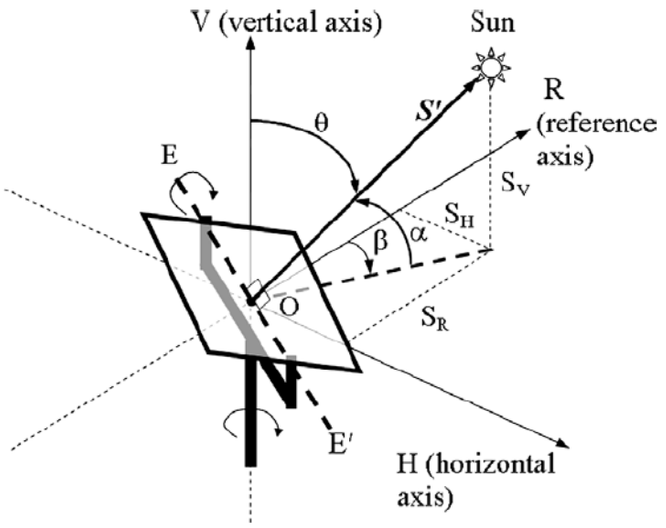

Fig. 4. In the collector-centre frame, the origin O is defined at the centre of the collector surface and it coincides with the origin of earth-surface frame. OV is defined as vertical axis in this coordinate system and it is parallel with first rotational axis of the solar collector. Meanwhile, OR is named as reference axis and the third orthogonal axis, OH, is named as horizontal axis. The OR and OH axes form the level plane where the collector surface is driven relative to this plane. The simplest structure of solar collector that can be driven in two rotational axes: the first rotational axis that is parallel with OV and the second rotational axis that is known as EE′ dotted line (it can rotate around the first axis during the sun-tracking but must always remain perpendicular with the first axis). From the diagram, θ is the amount of rotational angle about EE′ axis measured from OV axis, whereas β is the amount of rotational angle about OV axis measured from OR axis. Furthermore, α is solar altitude angle in the collector-centre frame, which is expressed as $\pi/2 - \theta$

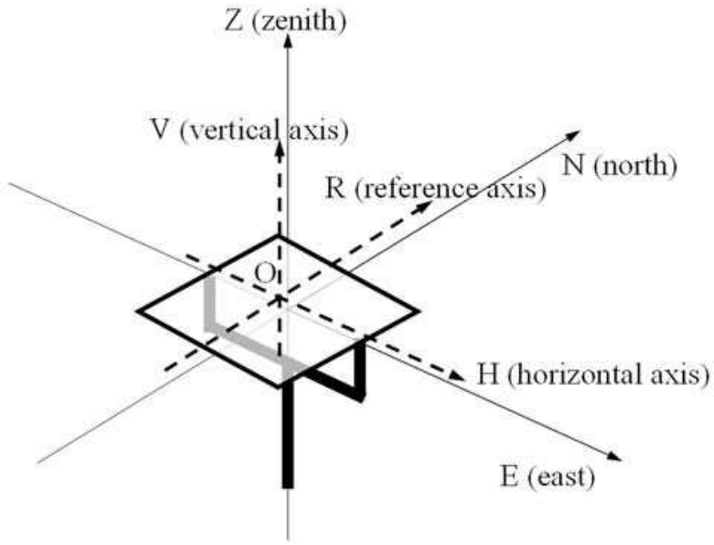

Fig. 5. In an ideal azimuth-elevation system, OV, OH and OR axes of the collector-centre frame are parallel with OZ, OE and ON axes of the earth-surface frame accordingly

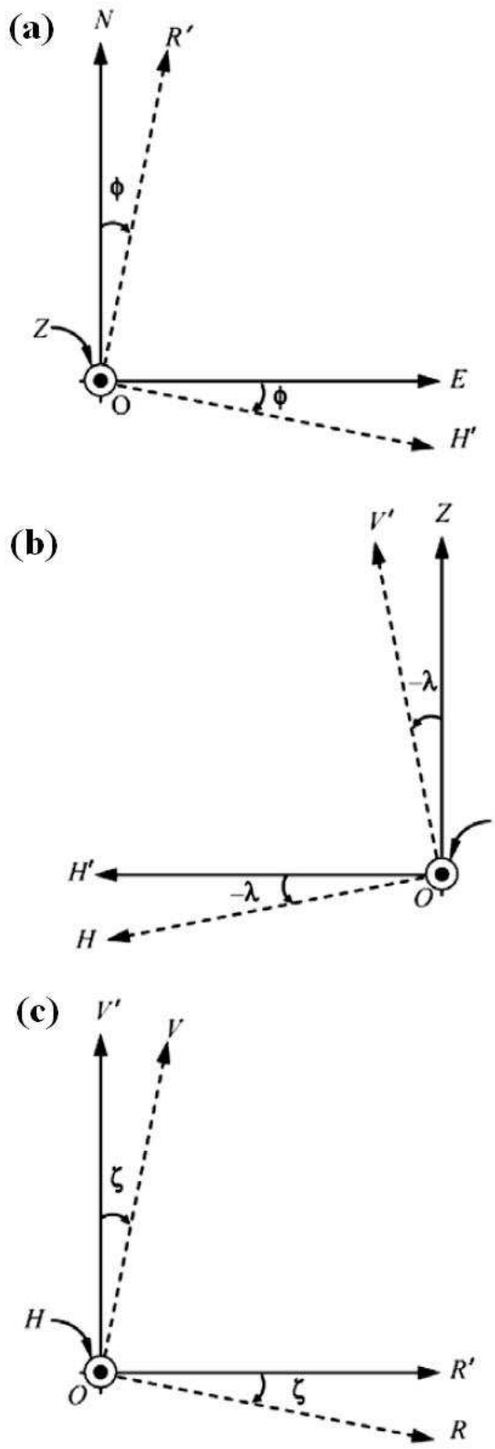

$$\begin{bmatrix} Z \\ H' \\ R' \end{bmatrix} = \begin{bmatrix} 1 & 0 & 0 \\ 0 & \cos\phi & -\sin\phi \\ 0 & \sin\phi & \cos\phi \end{bmatrix} \begin{bmatrix} Z \\ E \\ N \end{bmatrix}$$

$$\begin{bmatrix} V' \\ H \\ R' \end{bmatrix} = \begin{bmatrix} \cos\lambda & -\sin\lambda & 0 \\ \sin\lambda & \cos\lambda & 0 \\ 0 & 0 & 1 \end{bmatrix} \begin{bmatrix} Z \\ H' \\ R' \end{bmatrix}$$

$$\begin{bmatrix} V \\ H \\ R \end{bmatrix} = \begin{bmatrix} \cos\zeta & 0 & \sin\zeta \\ 0 & 1 & 0 \\ -\sin\zeta & 0 & \cos\zeta \end{bmatrix} \begin{bmatrix} V' \\ H \\ R' \end{bmatrix}$$

Fig. 6. The diagram shows the process of how the collector-centre frame is tilted step-by-step relative to the earth-surface frame, where OV′, OH′ and OR′ axes represent the intermediate position for OV, OH and OR axes, respectively. (a) The first tilted angle, $+\phi$, is a rotational angle about OZ-axis in clockwise direction in the first step of coordinate transformation

$$[\lambda]=\begin{bmatrix}\cos\lambda & -\sin\lambda & 0\\ \sin\lambda & \cos\lambda & 0\\ 0 & 0 & 1\end{bmatrix} \tag{6b}$$

$$[\zeta]=\begin{bmatrix}\cos\zeta & 0 & \sin\zeta\\ 0 & 1 & 0\\ -\sin\zeta & 0 & \cos\zeta\end{bmatrix} \tag{6c}$$

The new set of coordinates ***S′*** can be interrelated with the earth-centre frame based coordinate ***S*** through the process of four successive coordinate transformations. It will be first transformed from earth-centre frame to earth-surface frame through transformation matrix [Φ], then from earth-surface frame to collector-centre frame through three subsequent coordinate transformation matrices that are [ϕ], [λ] and [ζ]. In mathematical expression, ***S′*** can be obtained through multiplication of four successive rotational transformation matrices with ***S*** and it is written as

$$\begin{bmatrix}S_V\\ S_H\\ S_R\end{bmatrix} = [\zeta][\lambda][\phi][\Phi]\begin{bmatrix}\cos\delta\cos\omega\\ -\cos\delta\sin\omega\\ \sin\delta\end{bmatrix},$$

$$\begin{bmatrix}\sin a\\ \cos a\sin\beta\\ \cos a\cos\beta\end{bmatrix} = \begin{bmatrix}\cos\zeta & 0 & \sin\zeta\\ 0 & 1 & 0\\ -\sin\zeta & 0 & \cos\zeta\end{bmatrix}\times\begin{bmatrix}\cos\lambda & -\sin\lambda & 0\\ \sin\lambda & \cos\lambda & 0\\ 0 & 0 & 1\end{bmatrix}\times\begin{bmatrix}1 & 0 & 0\\ 0 & \cos\phi & -\sin\phi\\ 0 & \sin\phi & \cos\phi\end{bmatrix} \tag{7}$$
$$\times\begin{bmatrix}\cos\Phi & 0 & \sin\Phi\\ 0 & 1 & 0\\ -\sin\Phi & 0 & \cos\Phi\end{bmatrix}\times\begin{bmatrix}\cos\delta\cos\omega\\ -\cos\delta\sin\omega\\ \sin\delta\end{bmatrix}$$

Solving the above matrix equation for the solar altitude angle (α) in collector-frame, we have

$$\alpha=\arcsin\begin{bmatrix}\cos\delta\cos\omega\left(\cos\zeta\cos\lambda\cos\Phi-\cos\zeta\sin\lambda\sin\phi\sin\Phi-\sin\zeta\cos\phi\sin\Phi\right)\\ -\cos\delta\sin\omega\left(\sin\zeta\sin\phi-\cos\zeta\sin\lambda\cos\phi\right)\\ +\sin\delta\left(\cos\zeta\cos\lambda\sin\Phi+\cos\zeta\sin\lambda\sin\phi\cos\Phi+\sin\zeta\cos\phi\cos\Phi\right)\end{bmatrix} \tag{8}$$

Thus, the first tracking angle along EE′ axis is

$$\theta=\frac{\pi}{2}-\arcsin\begin{bmatrix}\cos\delta\cos\omega\left(\cos\zeta\cos\lambda\cos\Phi-\cos\zeta\sin\lambda\sin\phi\sin\Phi-\sin\zeta\cos\phi\sin\Phi\right)\\ -\cos\delta\sin\omega\left(\sin\zeta\sin\phi-\cos\zeta\sin\lambda\cos\phi\right)\\ +\sin\delta\left(\cos\zeta\cos\lambda\sin\Phi+\cos\zeta\sin\lambda\sin\phi\cos\Phi+\sin\zeta\cos\phi\cos\Phi\right)\end{bmatrix} \tag{9}$$

from earth-surface frame to collector-centre frame. (b) The second tilted angle, -λ, is a rotational angle about OR′ axis in counter-clockwise direction in the second step of coordinate transformation from earth-surface frame to collector-centre frame. (c) The third tilted angle, +ζ, is a rotational angle about OH axis in clockwise direction in the third step of coordinate transformation from earth-surface frame to collector-centre frame

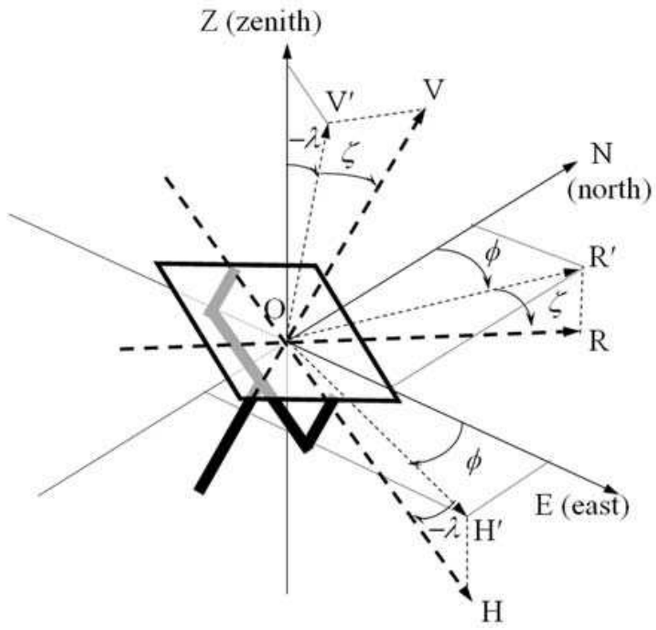

Fig. 7. The combination of the three rotations in 3D view from collector-centre frame to the earth-surface frame, where the change of coordinate system for each axis follows the order: $Z \to V' \to V$, $E \to H' \to H$ and $N \to R' \to R$

Similarly, the other two remaining equations that can be extracted from the above matrix equation expressed in cosine terms are as follow:

$$\sin\beta = \frac{\left[\begin{array}{c}\cos\delta\cos\omega\left(\sin\lambda\cos\Phi+\cos\lambda\sin\phi\sin\Phi\right)-\cos\delta\sin\omega\cos\lambda\cos\phi \\ +\sin\delta\left(\sin\lambda\sin\Phi-\cos\lambda\sin\phi\cos\Phi\right)\end{array}\right]}{\cos\alpha} \tag{10}$$

$$\cos\beta = \frac{\left[\begin{array}{c}\cos\delta\cos\omega\left(-\sin\zeta\cos\lambda\cos\Phi+\sin\zeta\sin\lambda\sin\phi\sin\Phi-\cos\zeta\cos\phi\sin\Phi\right) \\ -\cos\delta\sin\omega\left(\sin\zeta\sin\lambda\cos\phi+\cos\zeta\sin\phi\right) \\ +\sin\delta\left(-\sin\zeta\cos\lambda\sin\Phi-\sin\zeta\sin\lambda\sin\phi\cos\Phi+\cos\zeta\cos\phi\cos\Phi\right)\end{array}\right]}{\cos\alpha} \tag{11}$$

In fact, the second tracking angle along OV axis, β, can be in any of the four trigonometric quadrants depending on location, time of day and the season. Since the arc-sine and arc-cosine functions have two possible quadrants for their result, both equations of $\sin\beta$ and $\cos\beta$ require a test to ascertain the correct quadrant. Consequently, we have either

$$\beta = \arcsin\left[\frac{\begin{array}{c}\cos\delta\cos\omega\left(\sin\lambda\cos\Phi+\cos\lambda\sin\phi\sin\Phi\right)-\cos\delta\sin\omega\cos\lambda\cos\phi \\ +\sin\delta\left(\sin\lambda\sin\Phi-\cos\lambda\sin\phi\cos\Phi\right)\end{array}}{\cos\alpha}\right] \tag{12}$$

when $\cos\beta \geq 0$

or

$$\beta = \pi - \arcsin\left[\frac{\cos\delta\cos\omega\left(\sin\lambda\cos\Phi + \cos\lambda\sin\phi\sin\Phi\right) - \cos\delta\sin\omega\cos\lambda\cos\phi + \sin\delta\left(\sin\lambda\sin\Phi - \cos\lambda\sin\phi\cos\Phi\right)}{\cos\alpha}\right] \tag{13}$$

when $\cos\beta < 0$.

3.2 General formula for on-axis solar collector

The derived general sun-tracking formula is the most general form of solution for various kinds of arbitrarily oriented on-axis solar collector on the earth surface. In overall, all the on-axis sun-tracking systems fall into two major groups as shown in Fig. 1: (i) two-axis tracking system and (ii) one-axis tracking system. For two-axis tracking system, such as azimuth-elevation and tilt-roll tracking system, their tracking formulas can be derived from the general formula by setting different conditions to the parameters, such as ϕ, λ and ζ. In the case of azimuth-elevation tracking system, the tracking formula can be obtained by setting the angles $\phi = \lambda = \zeta = 0$ in the general formula. Thus, we can simplify the general formula to

$$\theta = \tfrac{\pi}{2} - \arcsin\left[\sin\delta\sin\Phi + \cos\delta\cos\omega\cos\Phi\right] \tag{14}$$

$$\beta = \arcsin\left[-\frac{\cos\delta\sin\omega}{\cos\alpha}\right] \tag{15}$$

when $\cos\beta \geq 0$
or

$$\beta = \pi - \arcsin\left[-\frac{\cos\delta\sin\omega}{\cos\alpha}\right] \tag{16}$$

when $\cos\beta < 0$
On the other hand, polar tracking method can also be obtained by setting the angles $\phi = \pi$, $\lambda = 0$ and $\zeta = \Phi - \pi/2$. For this case, the general tracking formula can be then simplified to

$$\theta = \pi/2 - \delta \tag{17}$$

$$\beta = \omega, \text{ when } -\pi/2 < \omega < \pi/2 \tag{18}$$

For one-axis tracking system, the tracking formula can be easily obtained from the full tracking formula by setting one of the tracking angles, which is either θ or β, as a constant value. For example, one of the most widely used one-axis tracking systems is to track the sun in latitude-tilted tracking axis. Latitude-tilted tracking axis is derived from tilt-roll tracking system with θ to be set as $\pi/2$ and the solar collector only tracks the sun with the angle $\beta = \omega$.

3.3 Application of general formula in improving sun-tracking accuracy

General sun-tracking formula not only provides the general mathematical solution for the case of on-axis solar collector, but also gives the ability to improve the sun-tracking accuracy by compensating the misalignment of the azimuth axis during the solar collector installation work. According to the general formula, the sun-tracking accuracy of the system is highly reliant on the precision of the input parameters of the sun-tracking algorithm: latitude angle (Φ), hour angle (ω), declination angle (δ), as well as the three orientation angles of the tracking axes of solar concentrator, i.e., ϕ, λ and ζ. Among these values, local latitude, Φ, and longitude of the sun tracking system can be determined accurately with the latest technology such as a global positioning system (GPS). On the other hand, ω and δ are both local time dependent parameters as shown in the Eq. (2) and Eq. (3). These variables can be computed accurately with the input from precise clock that is synchronized with the internet timeserver. As for the three orientation angles (ϕ, λ and ζ), their precision are very much reliant on the care paid during the on-site installation of solar collector, the alignment of tracking axes and the mechanical fabrication. Not all these orientation angles can be precisely obtained due to the limitation of measurement tools and the accuracy of determination of the real north of the earth. The following mathematical derivation is attempted to obtain analytical solutions for the three orientation angles based on the daily sun-tracking error results induced by the misalignment of sun-tracking axes (Chong et al., 2009b).

From the Eq. (7), the unit vector of the sun, S', relative to the solar collector can be obtained from a multiplication of four successive coordinate transformation matrices, i.e., [Φ], [ϕ], [λ] and [ζ] with the unit vector of the sun, S, relative to the earth. Multiply the first three transformation matrices [ϕ], [λ] and [ζ], and then the last two matrices [Φ] with S as to obtain the following result:

$$\begin{bmatrix} \sin\alpha \\ \cos\alpha\sin\beta \\ \cos\alpha\cos\beta \end{bmatrix} = \begin{bmatrix} \cos\zeta\cos\lambda & -\cos\zeta\sin\lambda\cos\phi+\sin\zeta\sin\phi & \cos\zeta\sin\lambda\sin\phi+\sin\zeta\cos\phi \\ \sin\lambda & \cos\lambda\cos\phi & -\cos\lambda\sin\phi \\ -\sin\zeta\cos\lambda & \sin\zeta\sin\lambda\cos\phi+\cos\zeta\sin\phi & -\sin\zeta\sin\lambda\sin\phi+\cos\zeta\cos\phi \end{bmatrix} \times \begin{bmatrix} \cos\Phi\cos\delta\cos\omega+\sin\Phi\sin\delta \\ -\cos\delta\sin\omega \\ -\sin\Phi\cos\delta\cos\omega+\cos\Phi\sin\delta \end{bmatrix}. \tag{19}$$

From Eq. (19), we can further break it down into Eq. (20):

$$\sin\alpha = (\cos\Phi\cos\delta\cos\omega+\sin\Phi\sin\delta)(\cos\zeta\cos\lambda)+(-\cos\delta\sin\omega)(-\cos\zeta\sin\lambda\cos\phi+\sin\zeta\sin\phi) + (-\sin\Phi\cos\delta\cos\omega+\cos\Phi\sin\delta)(\cos\zeta\sin\lambda\sin\phi+\sin\zeta\cos\phi) \tag{20a}$$

$$\cos\alpha\sin\beta = (\cos\Phi\cos\delta\cos\omega+\sin\Phi\sin\delta)(\sin\lambda)+(-\cos\delta\sin\omega)(\cos\lambda\cos\phi) + (-\sin\Phi\cos\delta\cos\omega+\cos\Phi\sin\delta)(-\cos\lambda\sin\phi) \tag{20b}$$

$$\cos\alpha\cos\beta = (\cos\Phi\cos\delta\cos\omega+\sin\Phi\sin\delta)(-\sin\zeta\cos\lambda)+(-\cos\delta\sin\omega)(\sin\zeta\sin\lambda\cos\phi+\cos\zeta\sin\phi) + (-\sin\Phi\cos\delta\cos\omega+\cos\Phi\sin\delta)(-\sin\zeta\sin\lambda\sin\phi+\cos\zeta\cos\phi) \tag{20c}$$

The time dependency of ω and δ can be found from Eq. (20). Therefore, the instantaneous sun-tracking angles of the collector only vary with the angles ω and δ. Given three different local times LCT_1, LCT_2 and LCT_3 on the same day, the corresponding three hours angles ω_1, ω_2 and ω_3 as well as three declination angles δ_1, δ_2 and δ_3 can result in three elevation angles α_1, α_2 and α_3 and three azimuth angles β_1, β_2 and β_3 accordingly as expressed in Eqs. (20a)–(20c). Considering three different local times, we can actually rewrite each of the Eqs. (20a)–(20c) into three linear equations. By arranging the three linear equations in a matrix form, the Eqs. (20a)–(20c) can subsequently form the following matrices

$$\begin{bmatrix} \sin\alpha_1 \\ \sin\alpha_2 \\ \sin\alpha_3 \end{bmatrix} = \begin{bmatrix} \cos\Phi\cos\delta_1\cos\omega_1 + \sin\Phi\sin\delta_1 & -\cos\delta_1\sin\omega_1 & -\sin\Phi\cos\delta_1\cos\omega_1 + \cos\Phi\sin\delta_1 \\ \cos\Phi\cos\delta_2\cos\omega_2 + \sin\Phi\sin\delta_2 & -\cos\delta_2\sin\omega_2 & -\sin\Phi\cos\delta_2\cos\omega_2 + \cos\Phi\sin\delta_2 \\ \cos\Phi\cos\delta_3\cos\omega_3 + \sin\Phi\sin\delta_3 & -\cos\delta_3\sin\omega_3 & -\sin\Phi\cos\delta_3\cos\omega_3 + \cos\Phi\sin\delta_3 \end{bmatrix} \times \begin{bmatrix} \cos\zeta\cos\lambda \\ -\cos\zeta\sin\lambda\cos\phi + \sin\zeta\sin\phi \\ \cos\zeta\sin\lambda\sin\phi + \sin\zeta\cos\phi \end{bmatrix}. \tag{21a}$$

$$\begin{bmatrix} \cos\alpha_1\sin\beta_1 \\ \cos\alpha_2\sin\beta_2 \\ \cos\alpha_3\sin\beta_3 \end{bmatrix} = \begin{bmatrix} \cos\Phi\cos\delta_1\cos\omega_1 + \sin\Phi\sin\delta_1 & -\cos\delta_1\sin\omega_1 & -\sin\Phi\cos\delta_1\cos\omega_1 + \cos\Phi\sin\delta_1 \\ \cos\Phi\cos\delta_2\cos\omega_2 + \sin\Phi\sin\delta_2 & -\cos\delta_2\sin\omega_2 & -\sin\Phi\cos\delta_2\cos\omega_2 + \cos\Phi\sin\delta_2 \\ \cos\Phi\cos\delta_3\cos\omega_3 + \sin\Phi\sin\delta_3 & -\cos\delta_3\sin\omega_3 & -\sin\Phi\cos\delta_3\cos\omega_3 + \cos\Phi\sin\delta_3 \end{bmatrix} \times \begin{bmatrix} \sin\lambda \\ \cos\lambda\cos\phi \\ -\cos\lambda\sin\phi \end{bmatrix}. \tag{21b}$$

$$\begin{bmatrix} \cos\alpha_1\cos\beta_1 \\ \cos\alpha_2\cos\beta_2 \\ \cos\alpha_3\cos\beta_3 \end{bmatrix} = \begin{bmatrix} \cos\Phi\cos\delta_1\cos\omega_1 + \sin\Phi\sin\delta_1 & -\cos\delta_1\sin\omega_1 & -\sin\Phi\cos\delta_1\cos\omega_1 + \cos\Phi\sin\delta_1 \\ \cos\Phi\cos\delta_2\cos\omega_2 + \sin\Phi\sin\delta_2 & -\cos\delta_2\sin\omega_2 & -\sin\Phi\cos\delta_2\cos\omega_2 + \cos\Phi\sin\delta_2 \\ \cos\Phi\cos\delta_3\cos\omega_3 + \sin\Phi\sin\delta_3 & -\cos\delta_3\sin\omega_3 & -\sin\Phi\cos\delta_3\cos\omega_3 + \cos\Phi\sin\delta_3 \end{bmatrix} \times \begin{bmatrix} -\sin\zeta\cos\lambda \\ \sin\zeta\sin\lambda\cos\phi + \cos\zeta\sin\phi \\ -\sin\zeta\sin\lambda\sin\phi + \cos\zeta\cos\phi \end{bmatrix}. \tag{21c}$$

where the angles Φ, ϕ, λ and ζ are constants with respect to the local time.

In practice, we can measure the sun tracking angles i.e. (α_1, α_2, α_3) and (β_1, β_2, β_3) during sun-tracking at three different local times via a recorded solar image of the target using a CCD camera. With the recorded data, we can compute the three arbitrary orientation angles (ϕ, λ and ζ) of the solar collector using the third-order determinants method to solve the three simultaneous equations as shown in Eqs. (21a)–(21c). From Eq. (21b), the orientation angle λ can be determined as follows:

$$\lambda = \sin^{-1}\left(\frac{\begin{vmatrix} \cos\alpha_1\sin\beta_1 & -\cos\delta_1\sin\omega_1 & -\sin\Phi\cos\delta_1\cos\omega_1 + \cos\Phi\sin\delta_1 \\ \cos\alpha_2\sin\beta_2 & -\cos\delta_2\sin\omega_2 & -\sin\Phi\cos\delta_2\cos\omega_2 + \cos\Phi\sin\delta_2 \\ \cos\alpha_3\sin\beta_3 & -\cos\delta_3\sin\omega_3 & -\sin\Phi\cos\delta_3\cos\omega_3 + \cos\Phi\sin\delta_3 \end{vmatrix}}{\begin{vmatrix} \cos\Phi\cos\delta_1\cos\omega_1 + \sin\Phi\sin\delta_1 & -\cos\delta_1\sin\omega_1 & -\sin\Phi\cos\delta_1\cos\omega_1 + \cos\Phi\sin\delta_1 \\ \cos\Phi\cos\delta_2\cos\omega_2 + \sin\Phi\sin\delta_2 & -\cos\delta_2\sin\omega_2 & -\sin\Phi\cos\delta_2\cos\omega_2 + \cos\Phi\sin\delta_2 \\ \cos\Phi\cos\delta_3\cos\omega_3 + \sin\Phi\sin\delta_3 & -\cos\delta_3\sin\omega_3 & -\sin\Phi\cos\delta_3\cos\omega_3 + \cos\Phi\sin\delta_3 \end{vmatrix}} \right) \tag{22a}$$

Similarly, the other two remaining orientation angles, ϕ and ζ can be resolved from Equation (21b) and Equation (21c) respectively as follows:

$$\phi = -\sin^{-1}\left(\frac{\begin{vmatrix} \cos\Phi\cos\delta_1\cos\omega_1 + \sin\Phi\sin\delta_1 & -\cos\delta_1\sin\omega_1 & \cos\alpha_1\sin\beta_1 \\ \cos\Phi\cos\delta_2\cos\omega_2 + \sin\Phi\sin\delta_2 & -\cos\delta_2\sin\omega_2 & \cos\alpha_2\sin\beta_2 \\ \cos\Phi\cos\delta_3\cos\omega_3 + \sin\Phi\sin\delta_3 & -\cos\delta_3\sin\omega_3 & \cos\alpha_3\sin\beta_3 \end{vmatrix}}{\begin{vmatrix} \cos\Phi\cos\delta_1\cos\omega_1 + \sin\Phi\sin\delta_1 & -\cos\delta_1\sin\omega_1 & -\sin\Phi\cos\delta_1\cos\omega_1 + \cos\Phi\sin\delta_1 \\ \cos\Phi\cos\delta_2\cos\omega_2 + \sin\Phi\sin\delta_2 & -\cos\delta_2\sin\omega_2 & -\sin\Phi\cos\delta_2\cos\omega_2 + \cos\Phi\sin\delta_2 \\ \cos\Phi\cos\delta_3\cos\omega_3 + \sin\Phi\sin\delta_3 & -\cos\delta_3\sin\omega_3 & -\sin\Phi\cos\delta_3\cos\omega_3 + \cos\Phi\sin\delta_3 \end{vmatrix}} \times \frac{1}{\cos\lambda} \right) \quad (22b)$$

$$\zeta = -\sin^{-1}\left(\frac{\begin{vmatrix} \cos\alpha_1\cos\beta_1 & -\cos\delta_1\sin\omega_1 & -\sin\Phi\cos\delta_1\cos\omega_1 + \cos\Phi\sin\delta_1 \\ \cos\alpha_2\cos\beta_2 & -\cos\delta_2\sin\omega_2 & -\sin\Phi\cos\delta_2\cos\omega_2 + \cos\Phi\sin\delta_2 \\ \cos\alpha_3\cos\beta_3 & -\cos\delta_3\sin\omega_3 & -\sin\Phi\cos\delta_3\cos\omega_3 + \cos\Phi\sin\delta_3 \end{vmatrix}}{\begin{vmatrix} \cos\Phi\cos\delta_1\cos\omega_1 + \sin\Phi\sin\delta_1 & -\cos\delta_1\sin\omega_1 & -\sin\Phi\cos\delta_1\cos\omega_1 + \cos\Phi\sin\delta_1 \\ \cos\Phi\cos\delta_2\cos\omega_2 + \sin\Phi\sin\delta_2 & -\cos\delta_2\sin\omega_2 & -\sin\Phi\cos\delta_2\cos\omega_2 + \cos\Phi\sin\delta_2 \\ \cos\Phi\cos\delta_3\cos\omega_3 + \sin\Phi\sin\delta_3 & -\cos\delta_3\sin\omega_3 & -\sin\Phi\cos\delta_3\cos\omega_3 + \cos\Phi\sin\delta_3 \end{vmatrix}} \times \frac{1}{\cos\lambda} \right) \quad (22c)$$

Fig. 8 shows the flow chart of the computational program designed to solve the three unknown orientation angles of the solar collector: ϕ, λ and ζ using Eqs. (22a)–(22c). By providing the three sets of actual sun tracking angle α and β at different local times for a

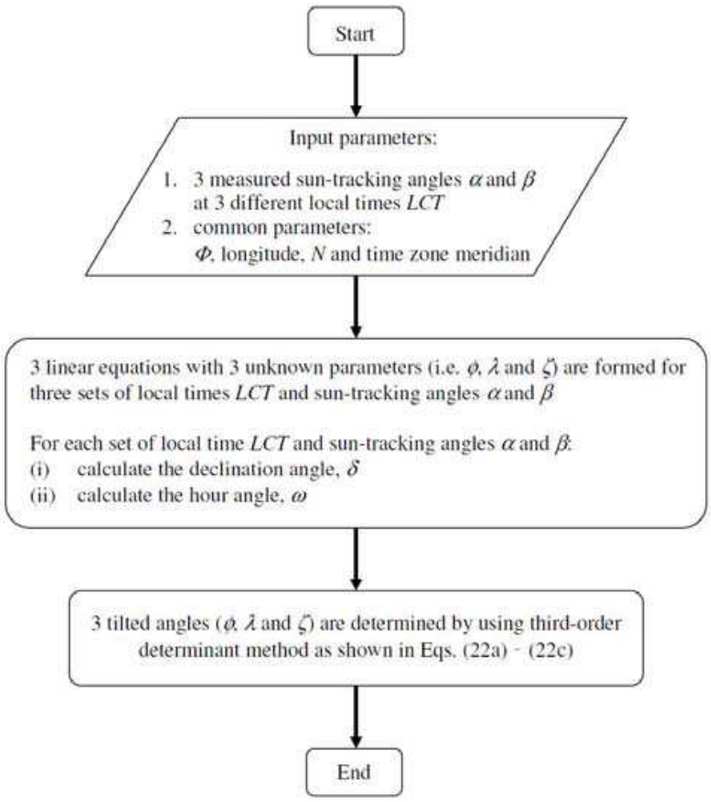

Fig. 8. The flow chart of the computational program to determine the three unknown orientation angles that cannot be precisely measured by tools in practice, i.e. ϕ, λ and ζ

particular number of day as well as geographical information i.e. longitude and latitude (Φ), the computational program can be executed to calculate the three unknown orientation angles (ϕ, λ and ζ).

4. Integration of general formula into open-loop sun-tracking system

4.1 Design and construction of open-loop sun-tracking system

For demonstrating the integration of general formula into open-loop sun-tracking control system to obtain high degree of sun-tracking accuracy, a prototype of on-axis Non-Imaging Planar Concentrator (NIPC) has been constructed in the campus of Univesiti Tunku Abdul Rahman (UTAR), Kuala Lumpur, Malaysia (located at latitude 3.22^o and longitude 101.73^o). A suitable geographical location was selected for the installation of solar concentrator so that it is capable of receiving the maximum solar energy without the blocking of any buildings or plants. The planar concentrator, applies the concept of non-imaging optics to concentrate the sunlight, has been proposed in order to achieve a good uniformity of the solar irradiation with a reasonably high concentration ratio on the target (Chong et al., 2009a; Chong et al., 2010). Instead of using a single piece of parabolic dish, the newly proposed on-axis solar concentrator employs 480 pieces of flat mirrors to form a total reflective area of about 25 m^2 with adjustable focal distance to concentrate the sunlight onto the target (see Fig. 9). The target is fixed at a focal point with a distance of 4.5 m away from the centre of solar concentrator frame.

Fig. 9. A prototype of 25m^2 on-axis Non-Imaging Planar Concentrator (NIPC) that has been constructed at Universiti Tunku Abdul Rahman (UTAR)

This planar concentrator is designed to operate on the most common two-axis tracking system, which is azimuth-elevation tracking system. The drive mechanism for the solar concentrator consists of stepper motors and its associated gears. Two stepper motors, with 0.72 degree in full step, are coupled to the shafts, elevation and azimuth shafts, with gear ratio of 4400 yielding an overall resolution of 1.64×10^{-4} °/ step. A Windows-based control program has been developed by integrating the general formula into the open-loop sun-tracking algorithm. In the control algorithm, the sun-tracking angles, i.e. azimuth (β) and elevation (α) angles, are first computed according to the latitude (Φ), longitude, day numbers (N), local time (LCT), time zone and the three newly introduced orientation angles (ϕ, λ and ζ). The control program then generate digital pulses that are sent to the stepper motor to drive the concentrator to the pre-calculated angles along azimuth and elevation movements in sequence. Each time, the control program only activates one of the two stepper motors through a relay switch. The executed control program of sun-tracking system is shown in Fig. 10.

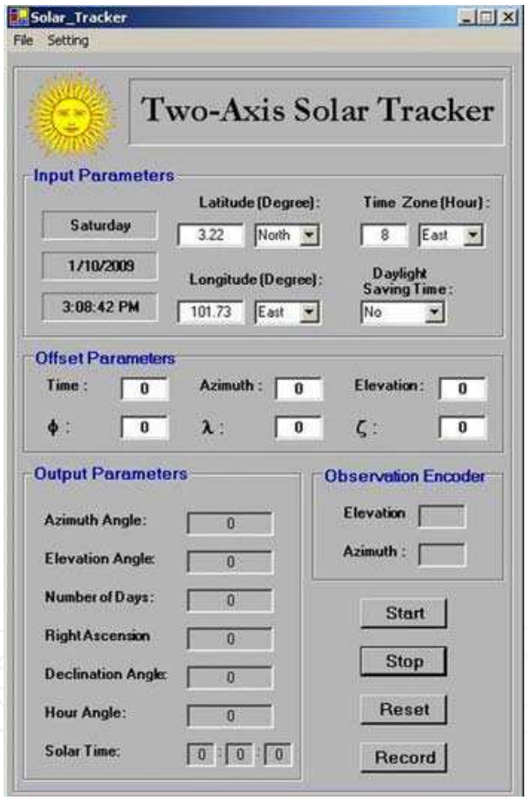

Fig. 10. A Windows-based control program that has been integrated with the on-axis general formula

An open-loop control system is preferable for the prototype solar concentrator to keep the design of the sun tracker simple and cost effective. In our design, open-loop sensors, 12-bit absolute optical encoders with a precision of 2,048 counts per revolution, are attached to the shafts along the azimuth and elevation axes of the concentrator to monitor the turning angles and to send feedback signals to the computer if there is any abrupt change in the encoder reading [see the inset of Fig. 11(b)]. Therefore, the sensors not only ensure that the

instantaneous azimuth and elevation angles are matched with the calculated values from the general formula, but also eliminate any tracking errors due to mechanical backlash, accumulated error, wind effects and other disturbances to the solar concentrator. With the optical encoders, any discrepancy between the calculated angles and real time angles of solar concentrator can be detected, whereby the drive mechanism will be activated to move the solar concentrator to the correct position. The block diagram and schematic diagram for the complete design of the open-loop control system of the prototype are shown in Fig. 11 (a), (b) respectively.

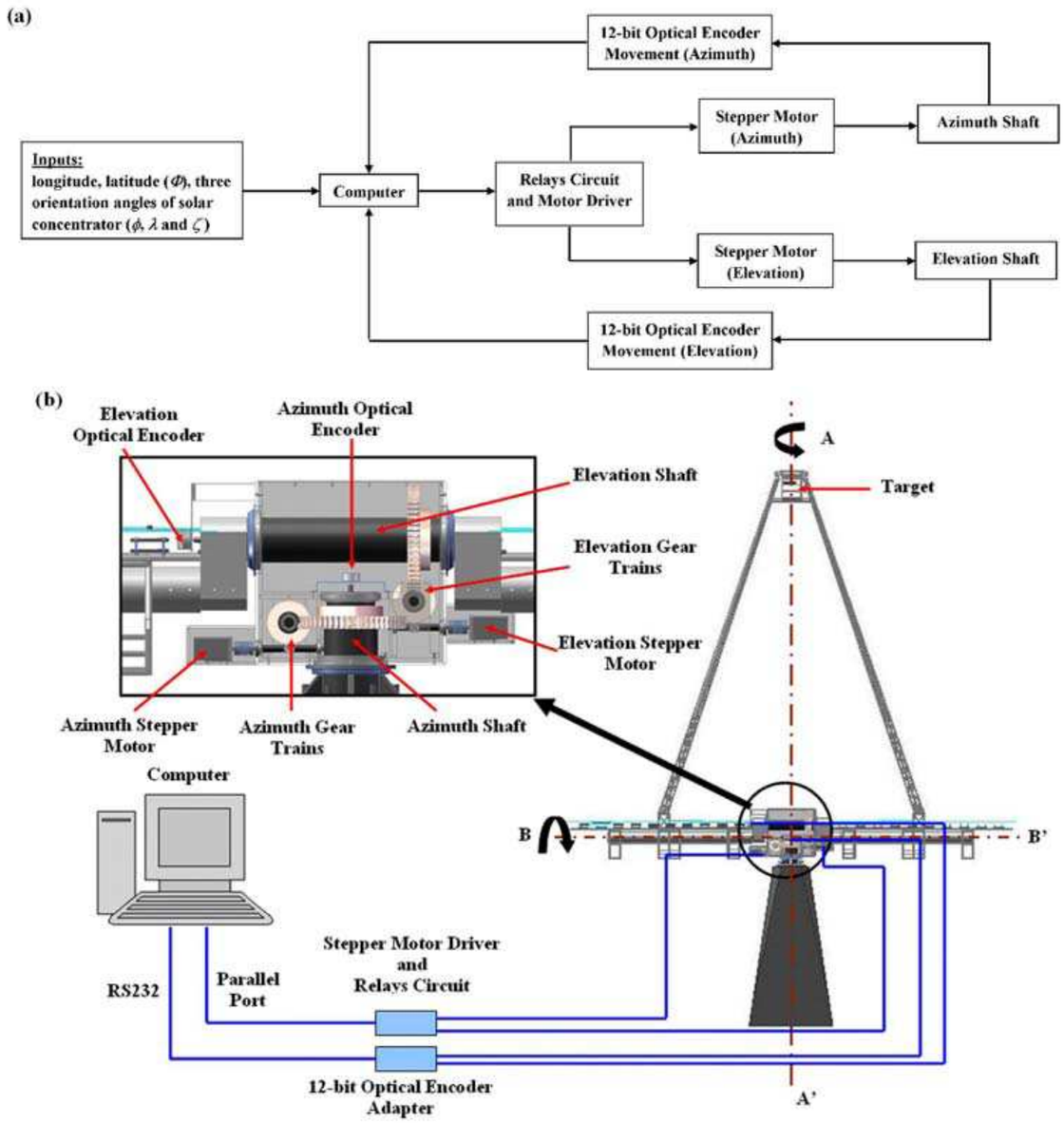

Fig. 11. (a) Block diagram to show the complete open-loop feedback system of the solar concentrator. (b) Schematic diagram to show the detail of the open-loop sun-tracking system of the prototype planar concentrator where AA' is azimuth-axis and BB' is elevation-axis.

4.2 Energy consumption

The estimated total electrical energy produced by the prototype solar concentrator and the total energy consumption by the sun-tracking system are also calculated. Taking into account of the total mirror area of 25 m², optical efficiency of 85%, and the conversion efficiency from solar energy to electrical energy of 30% for direct solar irradiation of 800 W/m², we have obtained the generated output energy of 35.7 kW-h/day for seven hours daily sunshine. Table 1 shows the energy consumption of 1.26 kW-h/day for the prototype includes the tracking motors, motor driver, encoders and computer. It corresponds to less than 3.5 % of the rated generated output energy. Among all these components, computer consumes the most power (more than 100W) and in future microcontroller can be used to replace computer as to reduce the energy consumption.

Total rotational angles of Elevation axis (degree/ day)	240
Total rotational angles of Azimuth axis (degree/ day)	540
Motor's rotational speed (rpm)	120
Gear ratio	1: 4400
Solar concentrator's angular speed (degree per second)	0.16
Total time for Elevation axis rotation (hour/ day)	0.41
Total time for Azimuth axis rotation (hour/ day)	0.92
Total operating time:10am-5pm (hour/ day)	7
Elevation motor's power consumption (watt)	99
Azimuth motor's power consumption (watt)	66
Power consumption of computer, encoders & motor driver (watt)	165
Energy Consumption of the Elevation motor (kW-h/day)	0.04
Energy Consumption of the Azimuth motor (kW-h/day)	0.06
Energy Consumption of computer, encoder & driver (kW-h/day)	1.16
Total Energy Consumption of the motors (kW-h/day)	1.26

Table 1. Specification and energy consumption of prototype sun-tracking system

5. Performance study and results

Before the performance of sun-tracking system was tested, all the mirrors are covered with black plastic (see Fig. 9), except the one mirror located nearest to the centre of the concentrator frame. To study the performance of the sun-tracking system, a CCD camera with 640 × 480 pixels resolution is utilized to capture the solar image cast on the target, which has a dimension of 60 cm × 60 cm and with a thickness of 1 cm steel plate, drawn with

28 cm × 26 cm target area. The camera is connected to a computer via a Peripheral Component Interconnect (PCI) video card as to have a real time transmission and recording of solar image. For the sake of accuracy, the CCD camera is placed directly facing the target to avoid the Cosine Effect. By observing the movement of the solar image via CCD camera, the sun-tracking accuracy can be analysed and recorded in the computer database every 30 minutes from 10 a.m. to 5 p.m. local time. Three different performance studies were executed in the year of 2009.

Study no. 1: First performance study has been carried out on 13 January 2009. Initially, we assume that the alignment of solar concentrator is perfectly done relative to real north and zenith by setting the three orientation angles as $\phi = \lambda = \zeta = 0°$ in the control program. According to the recorded results as shown in Fig. 12, the recorded tracking errors, ranging from 12.12 to 17.54 mrad throughout the day, have confirmed that the solar concentrator is misaligned relative to zenith and real north. Fig. 13 illustrates the recorded solar images at different local times.

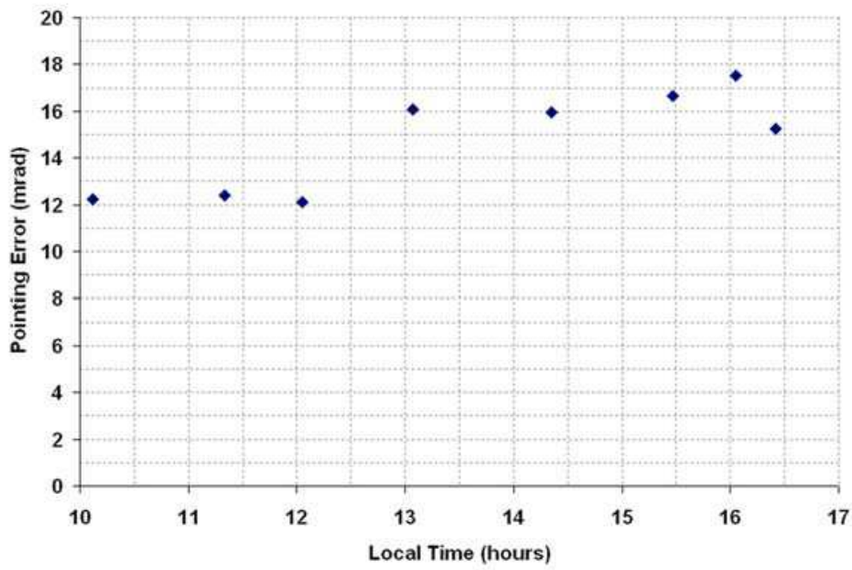

Fig. 12. The plot of pointing error (mrad) versus local time (hours) for the parameters, i.e. $\phi = \lambda = \zeta = 0°$, on 13 January 2009

Study no. 2: To rectify the problem of the sun-tracking errors due to imperfect alignment of the solar concentrator during the installation, we have to determine the three misaligned angles, i.e. ϕ, λ, ζ and then insert these values into the edit boxes provided by the control program as shown in Fig. 10. Thus, the computational program using the methodology as described in Fig. 8 was executed to compute the three new orientation angles of the prototype based on the data captured on 13 January 2009. The actual sun-tracking angles, i.e. (α_1, α_2 , α_3) and (β_1, β_2, β_3) at three different local times, can be determined from the central point of solar image position relative to the target central point by using the ray-tracing method. Three sets of sun-tracking angles at three different local times from the previous data were used as the input values to the computational program for simulating the three unknown parameters of ϕ, λ and ζ. The simulated results are $\phi = -0.1°$, $\lambda = 0°$, and $\zeta = -0.5°$.

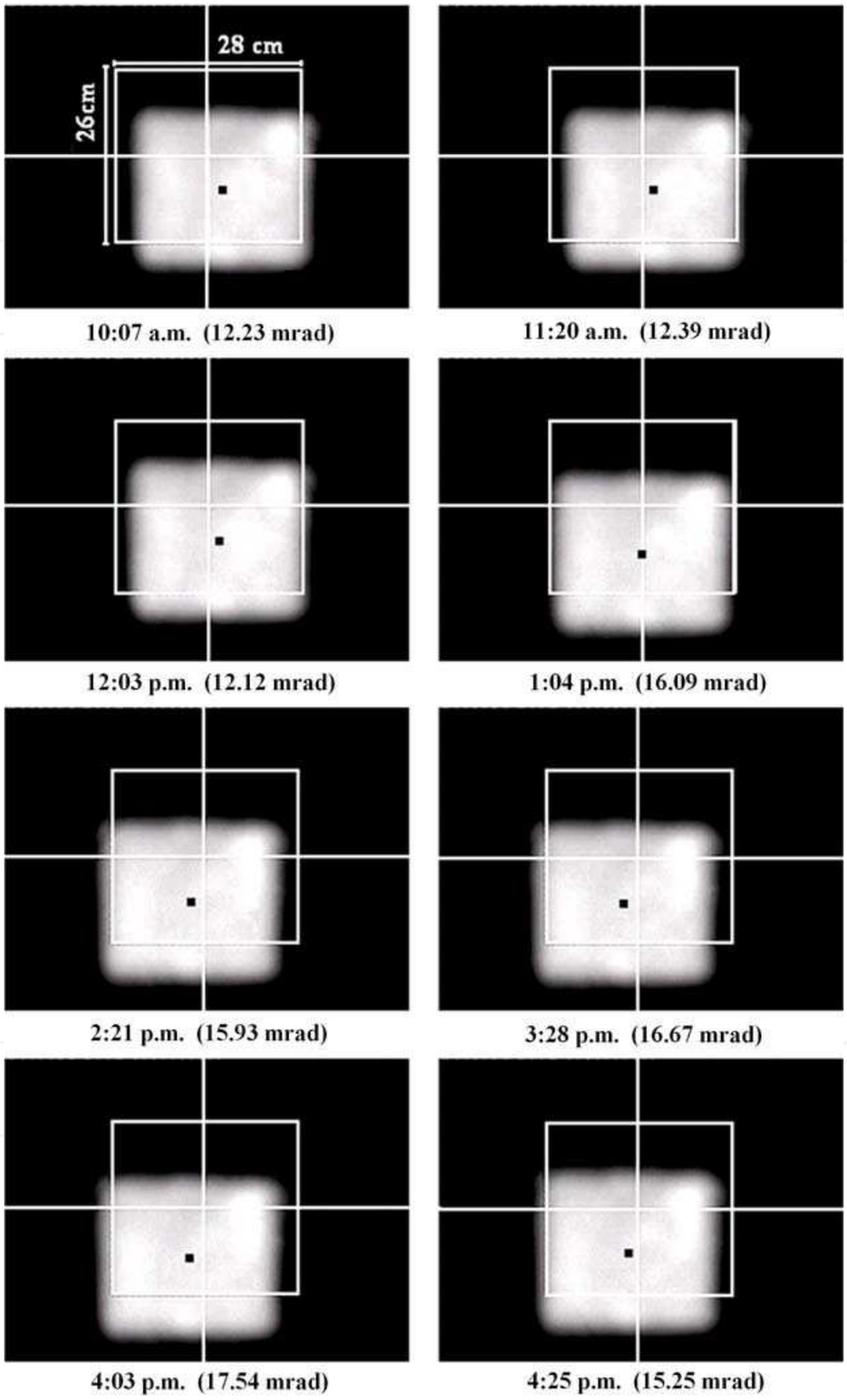

Fig. 13. The recorded solar images cast on the target of prototype solar concentrator using a CCD camera from 10:07 a.m. to 4:25 p.m. on 13 January 2009 with $\phi = \lambda = \zeta = 0°$

To substantiate the simulated results, these values were then used in the next session of sun-tracking that was performed on 16 January 2009. With the new orientation angles, the performance of the prototype in sun-tracking has been successfully improved to the accuracy of below 2.99 mrad, as shown in Fig. 14. It has reached the accuracy limit of the prototype as the optical encoder resolution that corresponds to 4.13 mrad, unless higher resolution of encoder is used for giving feedback signal. Fig. 15 shows the recorded solar images at the target for different local times ranging from 10 a.m. to 5 p.m. on 16 January 2009. In order to confirm the validation of the sun-tracking results, the sun-tracking system has been tested by running it for a period of more than six months.

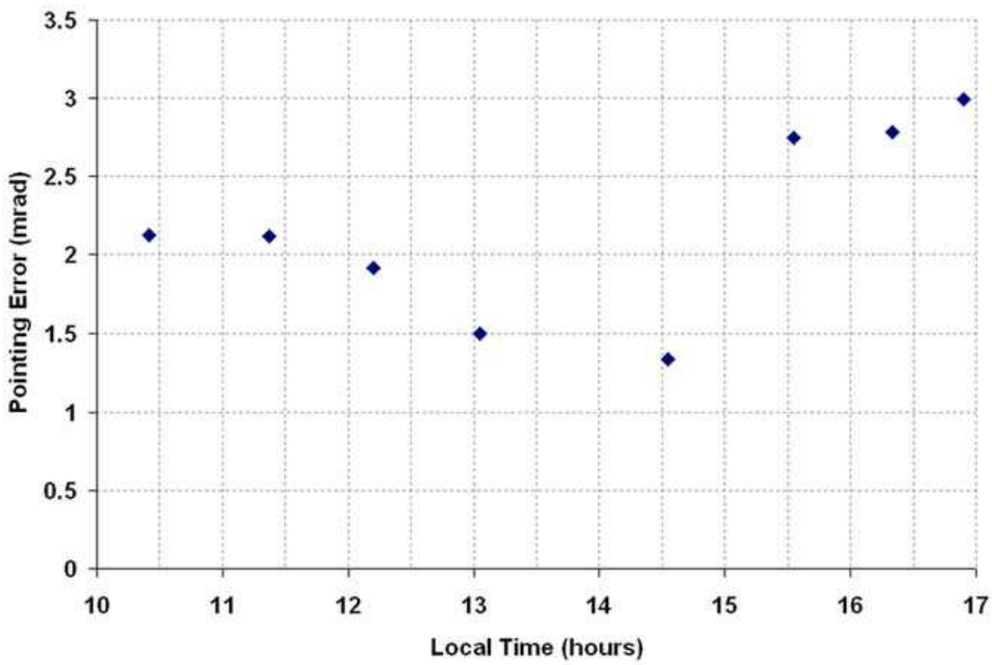

Fig. 14. The plot of pointing error (mrad) versus local time (hours) for the parameters, i.e. ϕ = −0.1°, λ = 0°, and ζ = −0.5°, on 16 January 2009

Study no. 3: On top of that, additional effort has been made to improve the sun-tracking accuracy beyond the resolution of the optical encoder by including the step count of stepper motor, 1.64 × 10^{-4} °/step, in fine-tuning the position of the prototype solar concentrator. Referring to the algorithm flow as shown in Fig. 16, the initial concentrator's azimuth and elevation angles are first defined with the reading of optical encoders, which are mounted on the azimuth and elevation axes respectively. Subsequently, the sun position angles, i.e. azimuth and elevation angles, are computed according to the general formula. The control program in succession compares the calculated sun angles with the current encoders' reading. If the absolute difference between the calculated azimuth or elevation angle and the encoder reading for azimuth or elevation axis (Δ_1) is larger than or equal to the encoder resolution, i.e. 0.176°, the control program then generates digital pulses that are sent to the stepper motor driver to drive the solar concentrator to the pre-calculated angles along azimuth and elevation axes in sequence with the use of relay switches, and stores the current reading of encoders as the latest concentrator's azimuth and elevation angles. In this

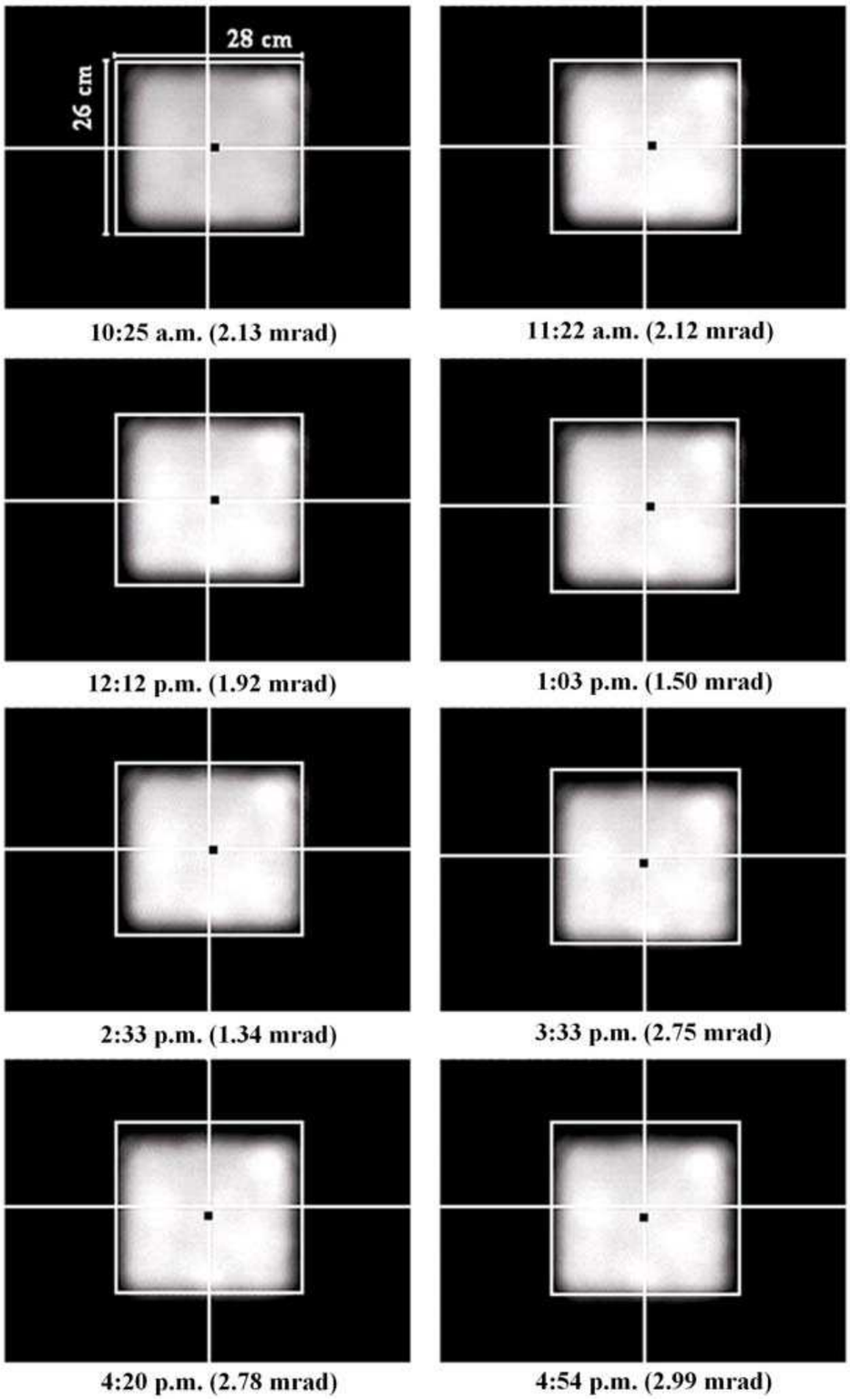

Fig. 15. The recorded solar images on the target of prototype solar concentrator using a CCD camera from 10:25 a.m. to 4:54 p.m. on 16 January 2009 with $\phi = -0.1°$, $\lambda = 0°$, and $\zeta = -0.5°$.

case, the program operates in feedback loop that is capable of making correction or compensating the disturbances like wind load and backlash so that the difference between the concentrator position angle and the calculated sun position angle is within the encoder resolution. Since the motor driving resolution (1.64×10^{-4} °/step) is far higher than the encoder resolution, a non-feedback loop has been introduced when the solar concentrator operates within the resolution of the optical encoder. In the non-feedback loop, we have included two assumptions in which backslash and step loss are negligible within the encoder resolution during the driving operation. When the absolute difference between the calculated azimuth or elevation angle and the concentrator's azimuth or elevation angles (Δ_2) is larger than or equal to 0.05° (this angle is sufficient for an on-axis solar concentrator to achieve a tracking accuracy of below 1 mrad), the control program will send the required pulses to motors for rotating the solar concentrator towards the sun along azimuth and elevation axes in order. After that, the timer is activated and the position of solar concentrator is updated with the sum of previous concentrator position angle and Δ_2. The solar concentrator is programmed to follow the sun at all times since the program is to run in repeated loops in every 10 seconds. Fig. 17 illustrates the pointing error (mrad) versus local time (hours) for different local times ranging from 10:00 a.m. to 4:10 p.m. on 6 August 2009 which has included the step count of stepper motor, 1.64×10^{-4} °/step. This strategy has further improved the tracking accuracy to 0.96 mrad on 6 August 2009 as shown in Fig. 18. Similarly, the performance of the sun-tracking has been observed for several months until end of year 2009.

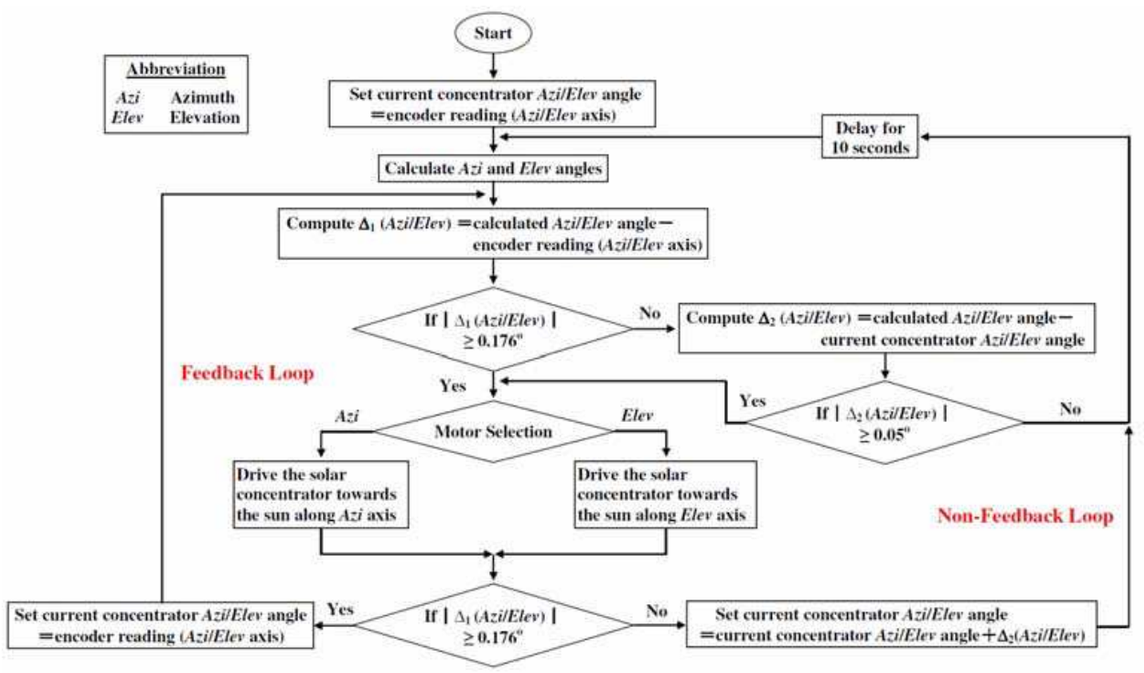

Fig. 16. The algorithm flow of the sun-tracking control program that including motor step count, 1.64×10^{-4} °/step, in fine-tuning the position of solar concentrator prototype and improving the sun tracking accuracy beyond the resolution of the optical encoder.

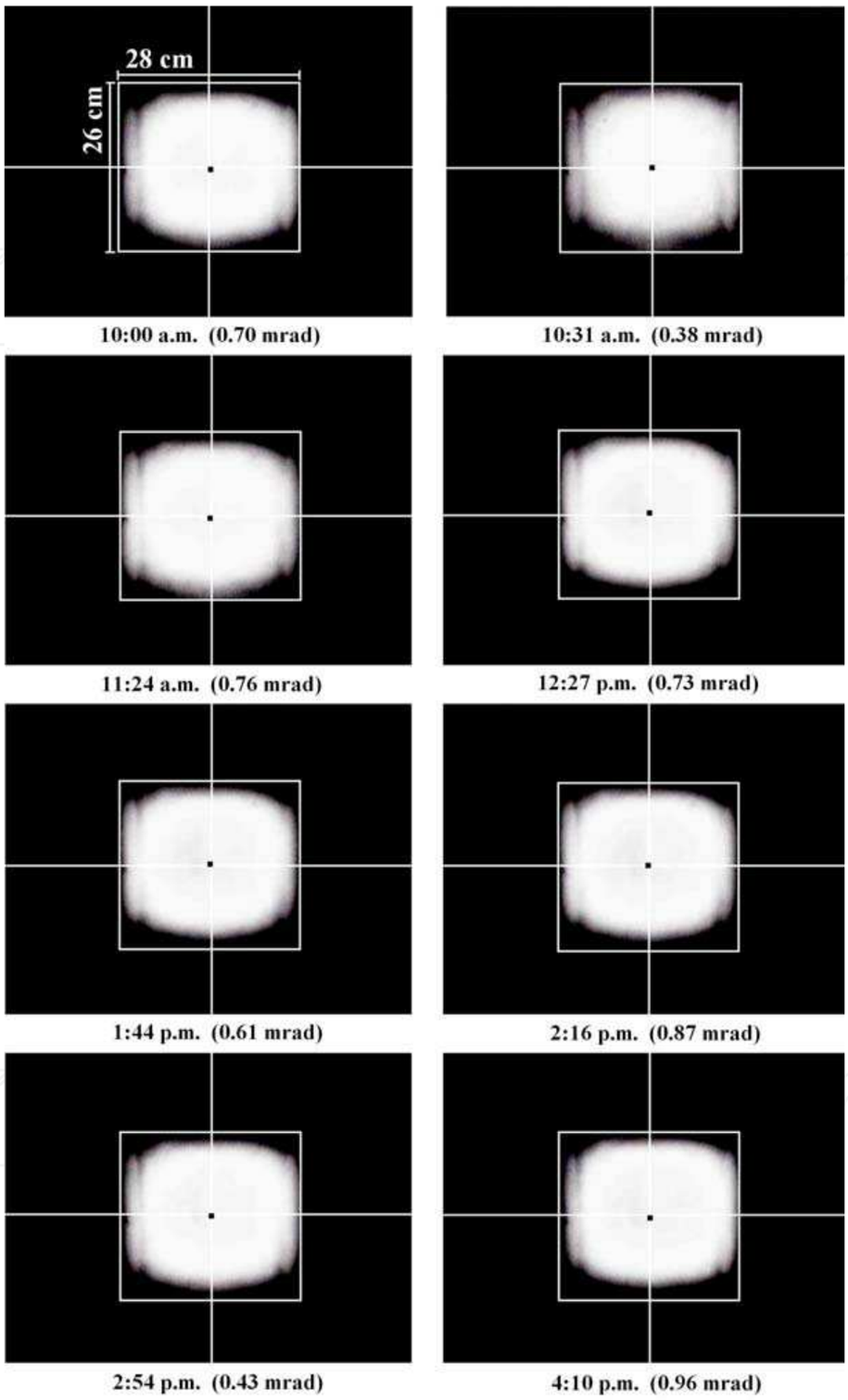

Fig. 17. The recorded solar images on the target of prototype solar concentrator using a CCD camera from 10:00 a.m. to 4:10 p.m. on 6 August 2009 with $\phi = -0.1°$, $\lambda = 0°$, and $\zeta = -0.5°$ and including the step count of stepper motor, 1.64×10^{-4} °/step

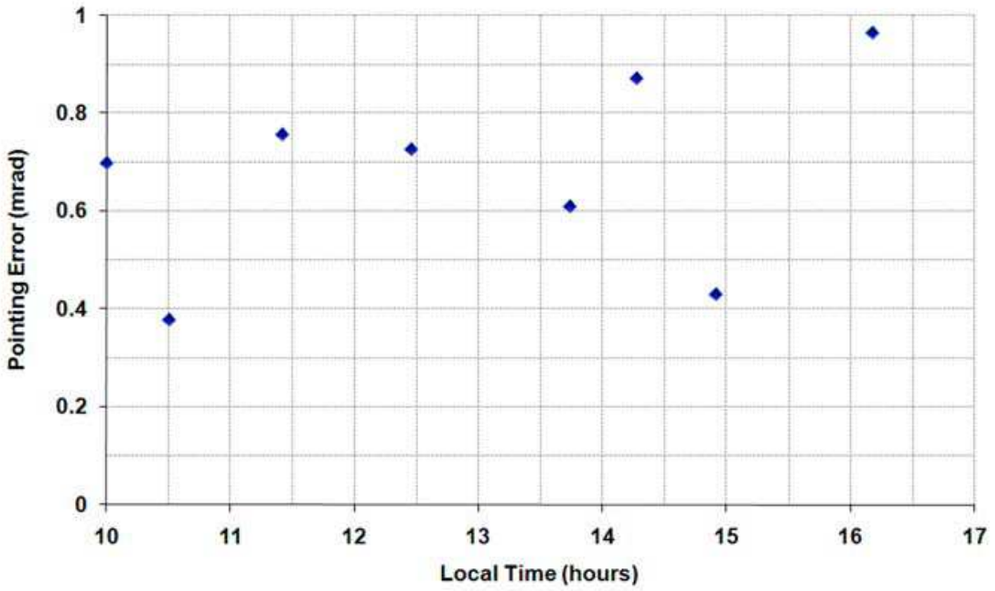

Fig. 18. The plot of pointing error (mrad) versus local time (hours) for the parameters, i.e. $\phi = -0.1°$, $\lambda = 0°$, and $\zeta = -0.5°$ on 6 August 2009 which has included the step count of stepper motor, 1.64×10^{-4} °/step

6. Conclusion

A novel on-axis general sun-tracking formula for various kinds of arbitrarily oriented on-axis solar collector has been derived using coordinate transformation method and integrated into the open-loop azimuth-elevation sun-tracking system intended for improving the tracking accuracy. In accordance with the experimental results, even though the misalignment on the azimuth axis relative to the zenith axis is within the range of 0.5 degree, the resulted sun-tracking error is significant, especially for the solar collector which requires high solar concentration and in particular for dense array concentrator photovoltaic (CPV) systems. With these results, the general sun-tracking formula is confirmed to be capable of rectifying the installation error of the solar concentrator with a significant improvement in the sun-tracking accuracy. In fact, there are many solutions of improving the tracking accuracy such as adding a closed-loop feedback system to the controller, designing a flexible mechanical platform that capable of two-degree-of-freedom for fine adjustment of azimuth shaft, etc. Nevertheless, all these solutions require a more complicated engineering design to the solar collector, which is also more complex and expensive. General sun-tracking formula allows the on-axis solar concentrator to track the sun accurately and simplifies the fabrication as well as the installation work of solar concentrator with higher tolerance in terms of the tracking axes alignment. Instead of using a complicated sun-tracking method, integrated on-axis general sun-tracking formula into the open-loop sun-tracking system is a clever method to get a reasonably high precision in sun-tracking with a much simple design and cost effective. This approach can significantly improve the performance and reduce the cost of solar energy collectors especially for high concentration systems.

7. References

Abdallah, S. & Nijmeh, S. (2004). Two axes sun tracking system with PLC control. *Energy Conversion and Management, Vol. 45, No. 11-12, (July* 2004) page numbers (1931-1939), ISSN 0196-8904

Aiuchi, K.; Yoshida, K.; Onozaki, M.; Katayama, Y.; Nakamura, M. & Nakamura, K. (2006). Sensor-controlled heliostat with an equatorial mount. *Solar Energy*, Vol.. *80, No. 9, (September 2006) page numbers (*1089-1097), ISSN 0038-092X

Arbab, H.; Jazi, B & Rezagholizadeh, M. (2009). A computer tracking system of solar dish with two-axis degree freedoms based on picture processing of bar shadow. *Renewable Energy, Vol. 34, No. 4, (April 2009) page numbers (*1114-1118), ISSN 0960-1481

Berenguel, M.; Rubio, F.R.; Valverde, A.; Lara, P.J.; Arahal, M.R.; Camacho, E.F. & Lopez, M. (2004). An artificial vision-based control system for automatic heliostat positioning offset correction in a central receiver solar power plant. *Solar Energy, Vol. 76, No. 5, (*2004) page numbers (563-575), ISSN 0038-092X

Blanco-Muriel, M.; Alarcon-Padilla, D.C.; Lopez-Moratalla, T. & Lara-Coira, M. (2001). Computing the solar vector. *Solar Energy, Vol. 70, No. 5, (*2001) page numbers (431-441), ISSN 0038-092X

Chen, F.; Feng, J. & Hong, Z. (2006). Digital sun sensor based on the optical vernier measuring principle. *Measurement Science and Technology, Vol. 17, No. 9, (September* 2006) page numbers (2494-2498), ISSN 0957-0233

Chen, F. & Feng, J. (2007). Analogue sun sensor based on the optical nonlinear compensation measuring principle. *Measurement Science and Technology, Vol. 18, No. 7, (July* 2007) number pages (2111-2115), ISSN 0957-0233

Chen, Y.T.; Chong, K.K.; Bligh, T.P.; Chen, L.C.; Yunus, J.; Kannan, K.S.; Lim, B.H.; Lim, C.S.; Alias, M.A.; Bidin, N.; Aliman, O.; Salehan, S.; Rezan S.A.H., S.A.; Tam, C.M. & Tan, K.K. (2001). Non-imaging, focusing heliostat. *Solar Energy, Vol. 71, No. 3, (*2001) page numbers (155-164), ISSN 0038-092X

Chen, Y.T.; Lim, B.H. & Lim, C.S. (2006). General sun tracking formula for heliostats with arbitrarily oriented axes. *Journal of Solar Energy Engineering,* Vol. 128, No. 2, (May 2006) page numbers (245-250), ISSN 0199-6231

Chong K.K. & Wong, C.W. (2009). General formula for on-axis sun-tracking system and its application in improving tracking accuracy of solar collector. *Solar Energy*, Vol. 83, No. 3, (March 2009) page numbers (298-305), ISSN 0038-092X

Chong, K.K.; Siaw, F.L.; Wong, C.W. & Wong G.S. (2009a). Design and construction of non-imaging planar concentrator for concentrator photovoltaic system. *Renewable Energy*, Vol. 34, No. 5, (May 2009) page numbers (1364-1370), ISSN 0960-1481

Chong, K.K.; Wong, C.W.; Siaw, F.L.; Yew, T.K.; Ng, S.S.; Liang, M.S.; Lim, Y.S. & Lau S.L. (2009b). Integration of an on-axis general sun-tracking formula in the algorithm of an open-loop sun-tracking system. *Sensors*, Vol. 9, No. 10, (September 2009) page numbers (7849-7865), ISSN 1424-8220

Chong, K.K.; Wong, C.W.; Siaw, F.L. & Yew, T.K. (2010). Optical characterization of nonimaging planar concentrator for the application in concentrator photovoltaic system. *Journal of Solar Energy Engineering*, Vol. 132, No. 1, (February 2010) page numbers (11011-11019), ISSN 0199-6231

Grena, R. (2008). An algorithm for the computation of the solar position. *Solar Energy*, Vol. 82, No. 5, (May 2008) page number (462-470), ISSN 0038-092X

Kalogirou, S.A. (1996). Design and construction of a one-axis sun-tracking system. *Solar Energy*, Vol. 57, No. 6, (December 1996) page number (465-469), ISSN 0038-092X

Kribus, A.; Vishnevetsky, I.; Yogev, A. & Rubinov, T. (2004). Closed loop control of heliostats. *Energy, Vol* 29, No. 5-6, (April-May 2004) page numbers (905-913), ISSN 0360-5442

Lee, C.D.; Yeh, H.Y.; Chen, M.H.; Sue, X.L. & Tzeng, Y.C. (2006). HCPV sun tracking study at INER. P*roceedings of the IEEE 4th World Conference on Photovoltaic Energy Conversion,pp. 718-720, ISBN* 1-4244-0017-1, Waikoloa Village, May 7-12 2006

Lee, C.Y.; Chou, P.C.; Chiang, C.M. & Lin, C.F. (2009). Sun Tracking Systems: A Review. *Sensors*, Vol. 9, No. 5, (May 2009) page numbers (3875-3890), ISSN 1424-8220

Luque-Heredia, I.; Gordillo, F.& Rodriguez, F. (2004). A *PI* based hybrid sun tracking algorithm for photovoltaic concentration. *Proceedings of the 19th European Photovoltaic Solar Energy Conversion,* Paris, France, June 7-14, 2004

Luque-Heredia, I.; Cervantes, R. & Quemere, G. (2006). A sun tracking error monitor for photovoltaic concentrators. P*roceedings of the IEEE 4th World Conference on Photovoltaic Energy Conversion,pp. 706-709, ISBN* 1-4244-0017-1, Waikoloa Village, USA, May 7-12 2006

Luque-Heredia, I.; Moreno, J.M.; Magalhaes, P.H.; Cervantes, R.; Quemere, G. & Laurent, O. (2007). Inspira's CPV sun tracking, In: *Concentrator Photovoltaics;* Luque, A.L. & Andreev, V.M., (Eds.), page numbers (221-251), Springer, ISBN 978-3-540-68796-2, Berlin, Heidelberg, Germany

Meeus, Jean. (1991). *Astronomical Algorithms*, Willmann-Bell, Inc., ISBN 0-943396-35-2, Virginia.

Nuwayhid, R.Y.; Mrad, F. & Abu-Said, R. (2001). The realization of a simple solar tracking concentrator for the university research applications. *Renewable Energy*, Vol. 24, No. 2, (October 2001) page numbers (207-222), ISSN 0960-1481

Reda, I. & Andreas, A. (2004). Solar position algorithm for solar radiation applications. *Solar Energy*, Vol. 76, No. 5, (2004) page number (577-589), ISSN 0038-092X

Rubio, F.R.; Ortega, M.G.; Gordillo, F. & Lopez-Martinez, M. (2007). Application of new control strategy for sun tracking. *Energy Conversion and Management, Vol. 48, No. 7, (July* 2007) page numbers (2174-2184), ISSN 0196-8904

Shanmugam, S. & Christraj, W. (2005). The tracking of the sun for solar paraboloidal dish concentrators. *Journal of Solar Energy Engineering*, Vol. 127, no. 1, (February 2005) page numbers (156-160), ISSN 0199-6231

Sproul, A.B. (2007). Derivation of the solar geometric relationships using vector analysis. *Renewable Energy*, Vol. 32, No. 7, (June 2007) page numbers (1187-1205), ISSN 0960-1481

Stine, W.B. & Harrigan, R.W. (1985). The sun's position. In: *Solar Energy Fundamentals and Design: With Computer Applications*, page numbers (38 – 69).John Wiley & Sons, Inc., ISBN 0-471-88718-8, New York

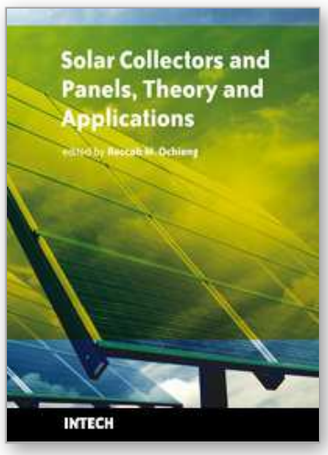

Solar Collectors and Panels, Theory and Applications

Edited by Dr. Reccab Manyala

ISBN 978-953-307-142-8
Hard cover, 444 pages
Publisher Sciyo
Published online 05, October, 2010
Published in print edition October, 2010

This book provides a quick read for experts, researchers as well as novices in the field of solar collectors and panels research, technology, applications, theory and trends in research. It covers the use of solar panels applications in detail, ranging from lighting to use in solar vehicles.

How to reference

In order to correctly reference this scholarly work, feel free to copy and paste the following:

Kok-Keong Chong and Chee-Woon Wong (2010). General Formula for On-Axis Sun-Tracking System, Solar Collectors and Panels, Theory and Applications, Dr. Reccab Manyala (Ed.), ISBN: 978-953-307-142-8, InTech, Available from: http://www.intechopen.com/books/solar-collectors-and-panels--theory-and-applications/general-formula-for-on-axis-sun-tracking-system

INTECH
open science | open minds

InTech Europe
University Campus STeP Ri
Slavka Krautzeka 83/A
51000 Rijeka, Croatia
Phone: +385 (51) 770 447
Fax: +385 (51) 686 166
www.intechopen.com

InTech China
Unit 405, Office Block, Hotel Equatorial Shanghai
No.65, Yan An Road (West), Shanghai, 200040, China
中国上海市延安西路65号上海国际贵都大饭店办公楼405单元
Phone: +86-21-62489820
Fax: +86-21-62489821

IntechOpen